7-20-2016

Three-dimensional architecture and hydrostratigraphy of cross-cutting buried valleys using airborne electromagnetics, glaciated Central Lowlands, Nebraska, USA

Jesse T. Korus Dr.

Robert Matthew Joeckel

Dana P. Divine

Jared D. Abraham

SEDIMENTOLOGY the journal of the International Association of Sedimentologists

Sedimentology (2017) **64**, 553–581 doi: 10.1111/sed.12314

Three-dimensional architecture and hydrostratigraphy of cross-cutting buried valleys using airborne electromagnetics, glaciated Central Lowlands, Nebraska, USA

JESSE T. KORUS*, R. MATT JOECKEL*†‡, DANA P. DIVINE* and JARED D. ABRAHAM§

**Conservation and Survey Division, School of Natural Resources, Institute of Agriculture and Natural Resources, University of Nebraska, Lincoln, NE, USA (E-mail: jkorus3@unl.edu)*

†Department of Earth and Atmospheric Sciences, University of Nebraska, Lincoln, NE, USA

‡University of Nebraska State Museum, University of Nebraska, Lincoln, NE, USA

§Aqua Geo Frameworks, LLC, Formerly with XRI Geophysics, LLC, Golden, CO, USA

Associate Editor – Nick Eyles

ABSTRACT

Buried valleys are characteristic features of glaciated landscapes, and their deposits host important aquifers worldwide. Understanding the stratigraphic architecture of these deposits is essential for protecting groundwater and interpreting sedimentary processes in subglacial and ice-marginal environments. The relationships between depositional architecture, topography and hydrostratigraphy in dissected, pre-Illinoian till sheets is poorly understood. Boreholes alone are inadequate to characterize the complex geology of buried valleys, but airborne electromagnetic surveys have proven useful for this purpose. A key question is whether the sedimentary architecture of buried valleys can be interpreted from airborne electromagnetic profiles. This study employs airborne electromagnetic resistivity profiles to interpret the three-dimensional sedimentary architecture of cross-cutting buried valleys in a *ca* 400 km^2 area along the western margin of Laurentide glaciation in North America. A progenitor bedrock valley is succeeded by at least five generations of tunnel valleys that become progressively younger northward. Tunnel-valley infills are highly variable, reflecting under-filled and over-filled conditions. Under-filled tunnel valleys are expressed on the modern landscape and contain fine sediments that act as hydraulic barriers. Over-filled tunnel valleys are not recognized in the modern landscape, but where they are present they form hydraulic windows between deep aquifer units and the land surface. The interpretation of tunnel-valley genesis herein provides evidence of the relationships between depositional processes and glacial landforms in a dissected, pre-Illinoian till sheet, and contributes to the understanding of the complex physical hydrology of glacial aquifers in general.

Keywords Airborne geophysics, buried valleys, glacial, hydrogeology, tunnel valleys.

INTRODUCTION

Buried valleys are ancient, channel-form stratigraphic features now buried by sediment or rock. Although the term 'buried valley' is commonly reserved for ancient valleys beneath and within glacial deposits (Cummings *et al.*, 2012), it applies also to ancient valleys (i.e. 'palaeovalleys' or 'incised valleys') in non-glaciated landscapes (Blum *et al.*, 2013). In the

present paper, the term refers to late Cenozoic glacial and non-glacial features near the western margin of Laurentide glaciation in North America that are filled with unconsolidated sediments. These buried valleys contain important high-yield aquifers, many of which are threatened by increasing water use, climate and land-use changes and pollution (Gosselin *et al.*, 1997; Druliner & Mason, 2001; Divine *et al.*, 2009). The sedimentary fills of buried valleys are typically heterogeneous and architecturally complex (e.g. Shaver & Pusc, 1992; Cummings *et al.*, 2012; Pugin *et al.*, 2014). Accurate characterization of the three-dimensional stratigraphic architecture is therefore essential in maximizing the efficient use of groundwater and for understanding pathways for contaminant transport. Furthermore, establishing the origins and genetic relationships of buried valleys within a broad framework of glacial and interglacial events contributes to a more comprehensive interpretation of sedimentary processes in subglacial and ice-marginal environments (Hooke & Jennings, 2006; Kehew *et al.*, 2012) and of late Cenozoic landscape evolution in central North America (Galloway *et al.*, 2011; Cummings *et al.*, 2012).

Quaternary buried valleys can be classified as: 'bedrock-interface valleys' or 'Quaternary sediment buried valleys' (Russell *et al.*, 2004). Bedrock-interface valleys are those that were eroded into bedrock but covered by Quaternary sediment. These valleys form via climatically driven or tectonically driven fluvial downcutting (Cummings *et al.*, 2012), incision by glacial meltwater streams or proglacial lake spillways (e.g. Kehew & Boettger, 1986), or erosion by subglacial meltwater (Fisher *et al.*, 2005; Kehew *et al.*, 2012; van der Vegt *et al.*, 2012). Quaternary sediment buried valleys are those that were both eroded into and covered by unconsolidated (Quaternary) deposits, and many formed as subglacial tunnels (e.g. Kehew *et al.*, 2012; Pugin *et al.*, 2014). These valleys commonly host inter-till aquifers (e.g. Cummings *et al.*, 2012), but they are difficult to map because valley-filling and valley-hosting strata often have similar lithologies. As a result, Quaternary sediment buried valleys typically escape scientific attention, although they may prove to be very important in understanding glacial sedimentology and hydrogeology. Further complicating matters, such buried valleys may actually be parts of the compound fills of larger, bedrock-interface valleys (Russell *et al.*, 2004).

Buried valleys (*sensu lato*) associated with ancient glacial episodes are extremely widespread in space and time; they have been documented on every continent and in association with Neoproterozoic, Ordovician and Permo-Carboniferous glaciations (van der Vegt *et al.*, 2012). Pleistocene buried valleys associated with glaciations in Europe have been studied intensively (e.g. Barker & Harker, 1984; Piotrowski, 1994; Gabriel *et al.*, 2003; Jørgensen *et al.*, 2003; Sandersen *et al.*, 2009; Janszen *et al.*, 2013) yet their equivalents in the interior of North America, although they too have socioeconomic importance, are much less well-known (e.g. Kehew & Boettger, 1986; Fisher & Taylor, 2002; Russell *et al.*, 2004; Ahmad *et al.*, 2009; Cummings *et al.*, 2012; Pugin *et al.*, 2014).

Pleistocene buried valleys, and probably some that date entirely or in part from the Pliocene (see discussion in Joeckel *et al.*, 2007), exist under much of the glaciated Central Lowlands of the United States and Canada. Their internal heterogeneities and sedimentary architectures, however, are typically not well-documented because subsurface data are limited and discontinuous. Most studies of buried valleys in North America have focused on Wisconsinan examples along the southern margin of the Laurentide Ice Sheet where well-preserved depositional topography can be used to interpret buried valley architecture and genesis (e.g. Fisher *et al.*, 2005; Räsänen *et al.*, 2009). Pre-Illinoian till sheets in North America, in contrast, are highly dissected (Fenneman, 1946), so surficial topography offers limited insight on subsurface architecture, if any at all. Although divides between modern drainage basins provide clues to the broad fabric of the pre-Illinoian glacial landscape (Lugn, 1935; Reed & Dreeszen, 1965), there has been very little independent evidence linking them to generations of buried valleys under or within till sheets. Such evidence is needed to advance the understanding of pre-Illinoian glacial–deglacial history in North America.

Characterizing the sedimentary architecture of complex glacial deposits can be quite challenging. Investigators often rely on lithological and geophysical data from closely spaced boreholes (e.g. Janszen *et al.*, 2013), outcrops (e.g. Slomka *et al.*, 2015), a combination of boreholes and outcrops (e.g. Boyce & Eyles, 2000) or, in some cases, ground-based, two-dimensional geophysical profiles supplemented by boreholes (e.g. Denne *et al.*, 1984; Jørgensen *et al.*, 2003; Abraham *et al.*, 2011). Resolving the intricate geometries and internal heterogeneities of buried valley

deposits requires spatially dense data suitable for three-dimensional reconstruction of sedimentary bodies. Recently, airborne electromagnetics (AEM) has been used successfully for 3D mapping of buried valleys in the glaciated areas of Denmark (Høyer *et al.*, 2015), Germany (Steuer *et al.*, 2009) and Canada (Pugin *et al.*, 2014). Despite these advances, much remains to be learnt from the interpretation of buried valley architecture from AEM data sets in a variety of settings, especially from pre-Illinoian glacial deposits. To date, little use has been made of sedimentary architecture for the interpretation of AEM data, primarily because bedding contacts are not resolvable in AEM when sediment bodies are lithologically uniform, and it can be difficult to account for multiple controlling variables on electrical properties in the subsurface (Lesmes & Friedman, 2005; Kirsch, 2009). However, this paper demonstrates that the sedimentary architecture of buried valleys in highly heterogeneous glacial deposits can be reconstructed in exquisite detail using AEM resistivity profiles.

The purposes of this study are: (i) to demonstrate the application of airborne electromagnetics to regional-scale 3D reconstructions of the architecture of complex buried valley fills under an old, dissected till sheet; (ii) to illuminate pre-Illinoian landscape evolution and deposystems near the western edge of the Laurentide Ice Sheet; and (iii) to provide an example of the characterization and the groundwater management implications of Quaternary buried valleys that can serve as a model for similar settings elsewhere.

GEOLOGICAL SETTING AND STUDY AREA

The study area lies in the glaciated Central Lowlands of North America near the overlap of the western margin of the Laurentide Ice Sheet on the High Plains aquifer (Fig. 1). There were at least seven glacial advances into the North American Midcontinent (including south-eastern Nebraska) between *ca* 2·6 Ma and *ca* 640 ka (Boellstorff, 1978a,b; Lanphere *et al.*, 2002; Roy *et al.*, 2004; Balco *et al.*, 2005). Modern streams are strongly oriented north or north-west to south or south-east. The drainage divides of major streams were interpreted as moraines by previous authors (Lugn, 1935; Reed & Dreeszen, 1965). Glacial deposits are mantled by a succession of loesses: the middle Pleistocene (Illinoian) Loveland Loess, the Gilman Canyon Formation (Wisconsinan) and the Late Pleistocene Peoria Loess. The Sangamon Geosol is developed locally at the top of the Loveland Loess (Fig. 2). Despite the widespread occurrence of glacial deposits, Quaternary sediment buried valleys have not previously been identified in eastern Nebraska.

At least five eastward-trending buried valleys have been identified on the bedrock surface in eastern Nebraska (Fig. 1; Dreeszen & Burchett, 1971). These buried valleys are traceable for >200 km from the unglaciated part of east-central Nebraska, where they form the base of the High Plains aquifer, to points as far eastward as south-western Iowa and north-western Missouri (Todd, 1911; Heim & Howe, 1963; Howe, 1968; Dreeszen & Burchett, 1971; Witzke & Ludvigson, 1990). These valleys follow the regional eastward slope of the landscape away from the Rocky Mountains, intersect the margin of the Laurentide Ice Sheet at *ca* 90°, and continue eastward beneath the glacial sediments (Dreeszen, 1970; Dreeszen & Burchett, 1971). The bedrock-interface valleys of south-east Nebraska are filled predominantly with sand and gravel and are buried by rolling, loess-mantled hills composed primarily of diamicton. Locally, the valley-fill sediments are either buried by stratified sands and silts within and beneath sheets of diamicton or they are cross-cut by modern stream valleys filled with Pleistocene and Holocene alluvium. Widely different origins have been proposed for these buried valleys. Reed & Dreeszen (1965) interpreted the buried valley sediments as proglacial deposits associated with the advancing Laurentide Ice Sheet. Emery (1966), Keech *et al.* (1967) and Ginsberg (1983) interpreted them as the products of the synglacial blockage of eastward-flowing streams during one or more glacial advances.

The valley-fill sediments constitute the principal aquifers in south-eastern Nebraska, providing water for irrigation, municipal, industrial and domestic uses (Divine *et al.*, 2009). These aquifers are truncated abruptly in many locations and their groundwater yields can vary considerably from place to place. Generalized hydrostratigraphic models constructed from widely spaced boreholes (e.g. Goodenkauf, 1978) have proven inadequate in attempts to predict the heterogeneity of these complex buried valleys.

The study area overlies the Dorchester-Sterling (DS) buried valley in southern Lancaster County, Nebraska (Fig. 1). This valley was eroded into Upper Pennsylvanian, Permian and Cretaceous bedrock (Fig. 2). Palaeozoic rocks consist of interbedded limestones, shales and mudstones,

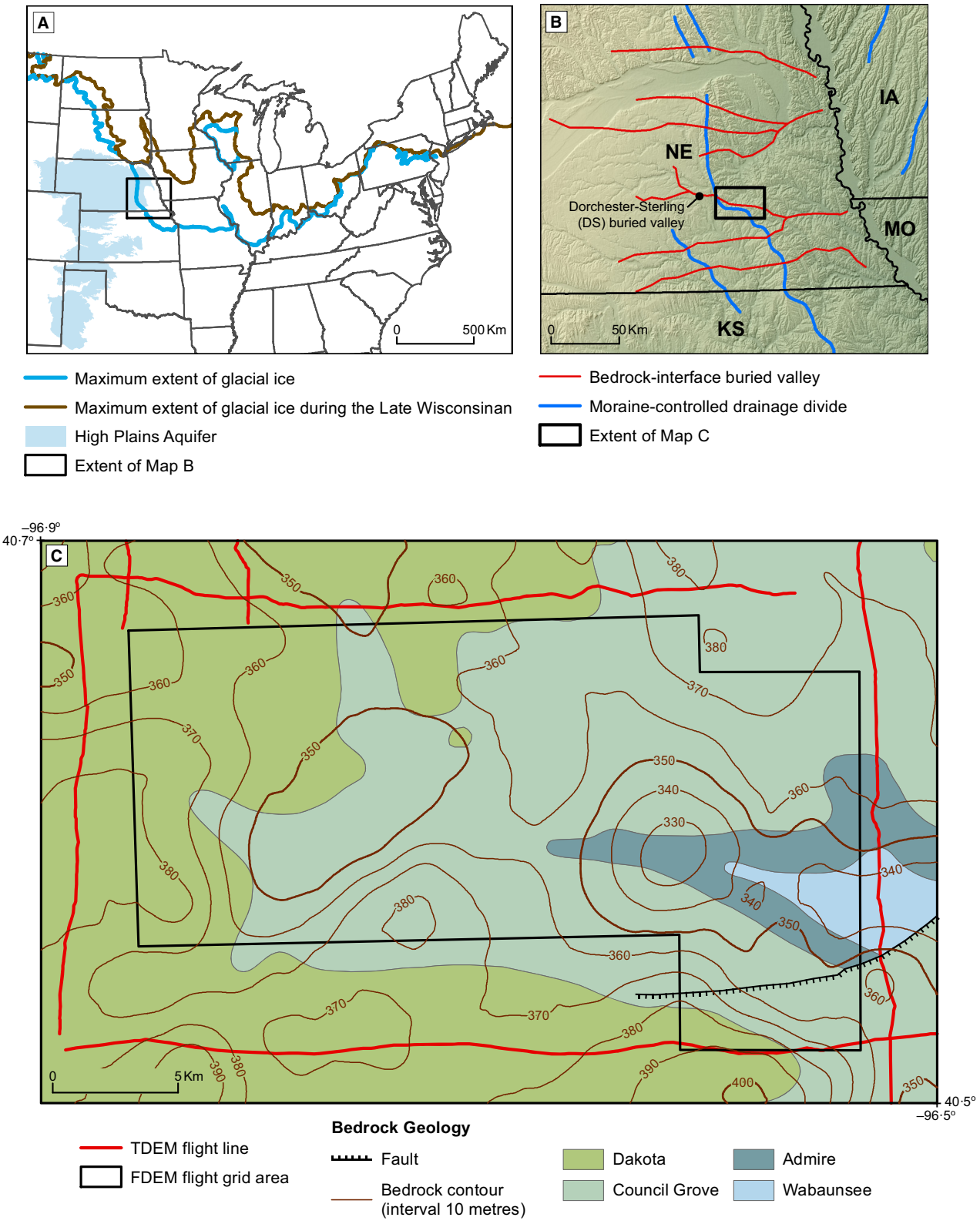

Fig. 1. Study area and principal geological features. (A) Maximum extent of pre-Illinoian and Wisconsinan glacial deposits. (B) South-eastern Nebraska and vicinity showing interpreted moraine-controlled drainage divides and bedrock-interface valleys. Topography from US Geological Survey National Elevation Data set (US Geological Survey, 2015). (C) Study area showing bedrock geology and elevation, frequency-domain electromagnetic (FDEM) block survey area and time-domain electromagnetic (TDEM) transects. Bedrock elevation contours from Divine (2014).

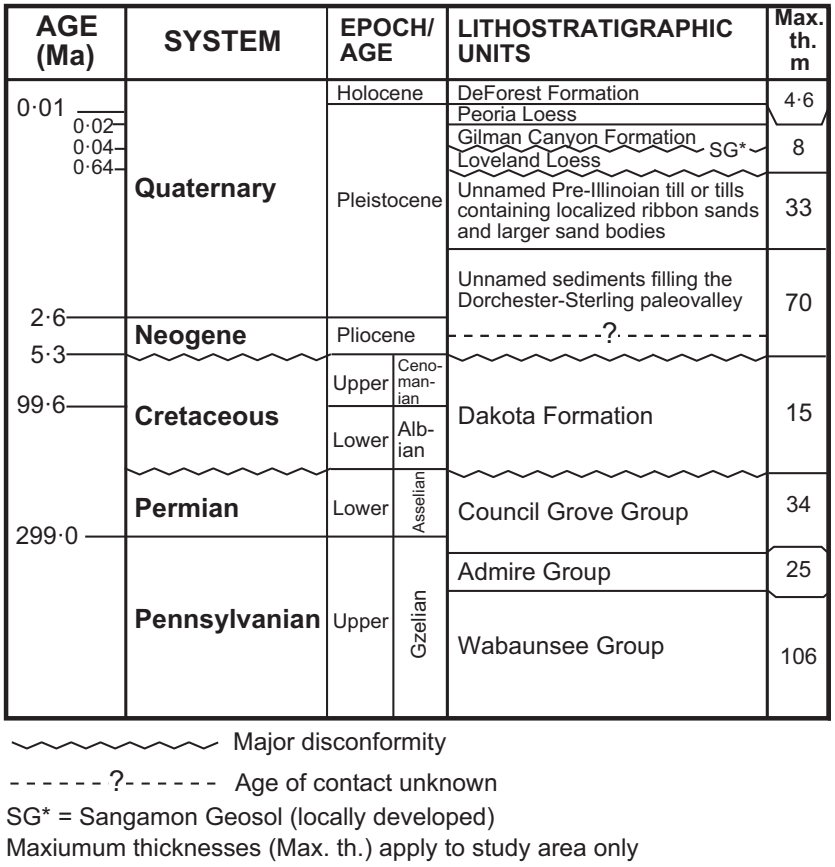

Fig. 2. Stratigraphic column of the study area.

which form the basal confining unit for all aquifers in the region. The Cretaceous Dakota Formation consists of sandstone, mudstone and shale, and it hosts a secondary aquifer that is important in parts of south-east Nebraska where buried valley aquifers are absent. The DS buried valley aquifer is an important source of water for a wide variety of uses, but management of the groundwater resource has proved challenging due to the complexity of the hosting sediments. Therefore, a detailed hydrogeological investigation was initiated in 2006. This study employed AEM surveys, and boreholes were drilled to target specific features revealed in AEM. The results of these studies are presented in Divine & Korus (2012) and Korus *et al.* (2013).

METHODS

Airborne electromagnetics

Airborne electromagnetic (AEM) investigations characterize the electrical properties of Earth materials using electromagnetic induction and can provide measurements from as shallow as 1 to 3 m in depth to as deep as 500 m. Typical AEM systems transmit an electromagnetic (radio-frequency) signal that interacts with Earth to induce secondary currents (Fig. 3). Those secondary currents are a function of the subsurface electrical resistivity, which is controlled by the amount of mineralogical clay, sediment texture, lithology, water content (concentration of dissolved solids), metallic mineralization and void space. Measurements of the secondary currents are recorded either in the frequency domain or in the time domain (explained below). In general, time-domain electromagnetic (TDEM) systems resolve subsurface properties at greater depths than frequency-domain electromagnetic (FDEM) systems, but FDEM systems have higher near-surface resolution. Depth sections of estimated electrical resistivity can be created along flight lines through numerical imaging and inversion, and interpolations between flight lines provide 3D views of electrical resistivity.

Frequency-domain airborne electromagnetics

Frequency-domain electromagnetic systems (FDEM) operate at fixed frequencies with three to six pairs of separated transmitter and receiver

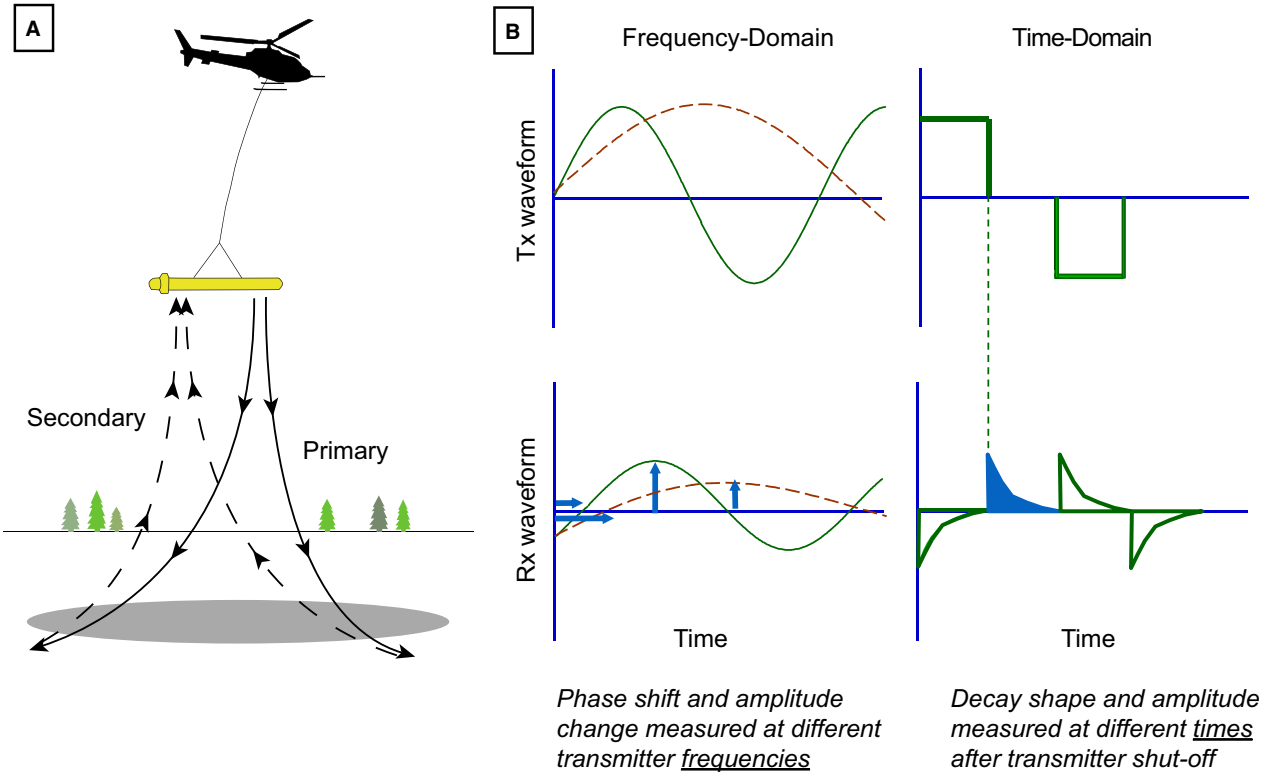

Fig. 3. Conceptualization of frequency-domain electromagnetic (FDEM) and time-domain electromagnetic (TDEM) methods. (A) General airborne electromagnetics (AEM) method with a sensor towed under a helicopter transmitting a primary signal that interacts with the earth materials producing a secondary signal that is received at the sensor. (B) Transmitted and received waveforms. Top illustrations are the transmitted (Tx) waveforms for both Frequency-Domain and Time-Domain waveforms. Lower illustrations are the received (Rx) waveforms.

coils that operate between 0·2 kHz and 140 kHz (Fig. 3). Lower frequencies are sensitive to greater depths. The system is towed *ca.* 30 m beneath a helicopter at average survey speeds of 30 m sec^{-1}, a ground clearance of 30 m, and at a nominal 280 m line spacing. Oscillating electrical currents in the transmitter coils induce secondary currents in the subsurface. The system of induced currents generates secondary magnetic fields that are picked up by the receiver coils, providing measurements of the electrical resistivity structure. At typical survey speeds, one sample of all frequencies is collected approximately every 3 m along the flight line. The footprint of the FDEM system along a survey line is *ca* 100 m, but this system footprint varies with frequency, survey altitude and resistivity (Beamish, 2003; Yin *et al.*, 2014). A six frequency system was used in this study, and is summarized in Smith *et al.* (2008, 2011).

Each sounding is converted to a one-dimensional profile of subsurface resistivity using a regularized least-squares inversion algorithm (Farquharson *et al.*, 2003). The use of a one-dimensional algorithm is only an approximation when structures are laterally heterogeneous over the footprint of the system, but such an application is defensible in the present study area because features of interest are larger than the FDEM system footprint. The ability to resolve targets is controlled by many factors: bandwidth of the measurement; power of the transmitter; height of the sensor; electrical conductivity of the earth materials; and the presence of man-made infrastructure (power lines, pipelines and train tracks). Highly conductive materials typically impact FDEM systems, which limit the effective depth of investigation (Abraham *et al.*, 2011). The process of numerical inversion also introduces a level of non-uniqueness in the results. The inversion process solves a model that best represents the FDEM data which were recorded over a section of the survey area. However, there are many solutions that can equally fit the data with the range of the data error. This is due to the noise in the data, the bandwidth of

the system and the setup of the model (number of layers, starting models). Maximum and minimum resistivity value constraints, based on examination of the local borehole resistivity logs, are put on the FDEM models to provide realistic boundaries for the inversions to produce reasonable geological results.

The vertical resolution of FDEM decreases with depth due to the increased wavelength of the lower frequencies. Resistivity values in the deepest parts of the profile are averaged over larger intervals than those in the shallowest part of the profile, so thin geological bodies are less likely to be resolved at depth. The maximum depth of investigation of FDEM in the vicinity of the test holes in this study varied from *ca* 55 m in areas where conductive sediments exist near the land surface to *ca* 75 m in areas dominated by resistive materials.

Time-domain airborne electromagnetics

Time-domain electromagnetic (TDEM) systems send an electrical current through a large loop of wire (transmitter or Tx coil) which generates an electromagnetic (EM) field (Fig. 3). Abrupt termination of the current causes the EM field to dissipate and decay, travelling deeper and spreading wider into the subsurface. The rate of dissipation is dependent on the electrical properties of the subsurface. At the moment the current is terminated, a secondary EM field, which also begins to decay, is generated within the subsurface. The decaying secondary EM field generates a current in a receiver (Rx) coil, which is measured at several different moments in time (time gates). From this current, the time rate of decay of the magnetic field is determined. When compiled in time, these measurements become a 'sounding' at that location.

A dual moment TDEM system was used in this study. This system is designed to overcome the difficulties imposed by use of large Tx coils, which are necessary to see deeper targets or to see through highly conductive materials. Specifics of the system that was used in this study are included in Carney *et al.* (2015).

As in the FDEM processing methods, the sounding curves generated by the TDEM surveys are numerically inverted to produce a model of subsurface resistivity as a function of depth. Inversion relates the measured geophysical data to probable physical earth properties. Noise, bandwidth and infrastructure impact the resolution and depth of investigation. The TDEM inversion process that was used in this study was a spatially constrained method that uses a one-dimensional model that is spatially constrained to adjacent sounding resistivity models providing a quasi-three-dimensional resistivity model (Viezzoli *et al.*, 2008).

The vertical resolution of TDEM is generally less than the frequency-domain systems, but is controlled by the bandwidth of the system and the modelling layers used in the inversion. For the inversions in this study area, the smallest model layer was 5 m at the top of the model and 40 m at the bottom of the 500 m model. Horizontal resolution is controlled by many factors including: acquisition, bandwidth of system, size of transmitter and spatial constraints of the inversion. For this study, the spatial sampling was *ca* 30 m. Reid & Vrbancich (2004) and Reid *et al.* (2006) provide insight into the impact of the bandwidth, height and electrical conductivity impacts on the system footprint. One additional impact on the horizontal and, to some extent, the vertical resolution, is the numerical regularizations that are put on the inversion. This includes the amount the inversions are able to change the resistivity from one sounding to the next. If the regularizations are too tight, the data could be over-smoothed and would not appropriately indicate the spatial changes from one sounding to the next. These regularization values are selected carefully after comparisons to boreholes and inspection of model versus data residuals. More information on the inversion of the TDEM data in this study can be found in Carney *et al.* (2015).

Field and laboratory methods

This study employs data from 21 pre-existing test holes, drillers' logs from 847 water wells and logs from 21 new test holes. The new test holes were sited carefully to target specific features and areas of interest revealed in AEM data. Auger-rig and mud-rotary systems were used. Cores were obtained from the uppermost *ca* 5 to 35 m of seven of the new test holes. Auger penetration was denied before reaching bedrock, so mud-rotary drilling was used at the same location to advance the test holes into bedrock. Cores and cuttings were described in the field initially, and then detailed descriptions were completed in the laboratory.

Selected core samples were analysed for sand, silt and clay fractions using a Malvern laser particle-size analyser (Malvern Instruments Limited, Malvern, UK). Gravel percentages were estimated based on gravel weight relative to total sample weight.

Gamma-ray (Gamma), 64 inch normal resistivity (Res64n), 16 inch normal resistivity (res16n), lateral resistivity (ResLat) and single-point resistivity logs were produced for the new test holes. A comparison with the results of Palacky & Stevens (1990) and Best *et al.* (2006) indicates that uncorrected resistivity values are still in the typical range for unconsolidated sediments. The logs are used herein for qualitative comparison to AEM because detailed calibration and corrections would need to be carried out for the resistivity values in the logs to be used directly as a numerical constraint in the inversion of the AEM data (Ley-Cooper and Davis, 2010). For example, two logs – one in an area of high resistivity (Fig. 4A) and one in an area of low-resistivity area (Fig. 4B) – are presented to illustrate the comparison of the AEM inversions to the uncalibrated logs. The recovered AEM resistivity model compares well with the two logs, indicating that the AEM resistivity models are imaging the resistivity contrasts within the study area. Furthermore, AEM resistivity at this study site does not appear to be controlled by factors such as degree of water saturation and groundwater chemistry. Korus *et al.* (2013) conducted a borehole by borehole comparison of water table position, groundwater chemistry and AEM resistivities. The analysis revealed that the resistivity contrast between saturated and unsaturated sands lies at a value greater than the 20 ohm-m cut-off value between fine and coarse sediments. It also revealed that changes in groundwater chemistry are not sufficient to impact AEM resistivity. Thus, regardless of the degree of water saturation or chemistry, sand and gravel can be distinguished very clearly from silt, clay and diamicton on the basis of electrical resistivity (Divine & Korus, 2012; Korus *et al.*, 2013).

Sedimentary architecture was investigated using 2D cross-sections showing the AEM resistivity-depth profiles, together with borehole data located within 100 to 200 m of the helicopter flight line. Bounding surfaces were digitized on 2D profiles and then were assembled into 3D

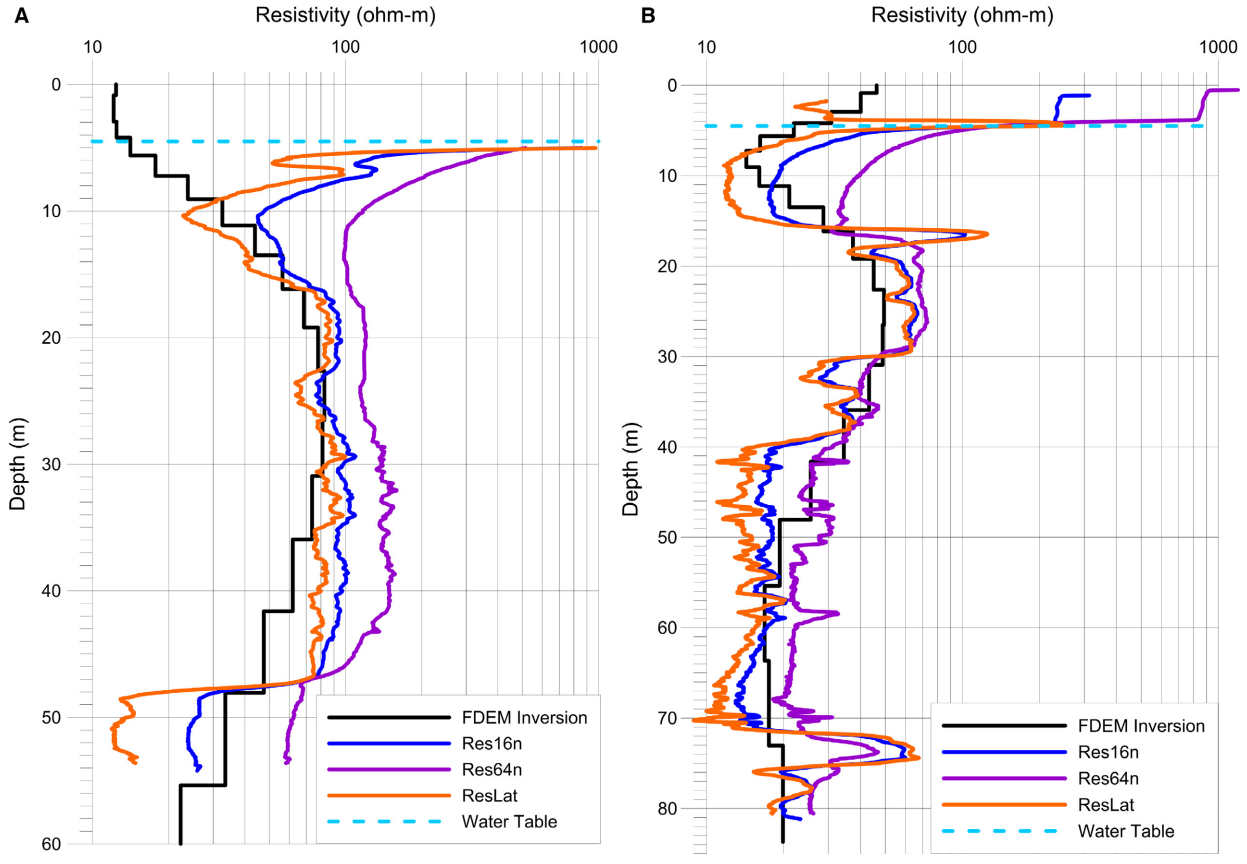

Fig. 4. Comparison of frequency-domain electromagnetic (FDEM) resistivity inversion models and geophysical logs at two locations. (A) Test hole 11-EN-07 (high resistivity area) with the FDEM inversion *ca* 70 m away from the test hole. (B) Test hole 4-EN-11 (low-resistivity area) with the AEM inversion *ca* 50 m away from the test hole.

interpretations by correlating between profiles spaced *ca* 280 m apart. The bedrock surface could not be mapped in FDEM profiles because: (i) the depth of bedrock exceeded the depth of investigation in most locations; and (ii) in those locations where the bedrock surface is within the depth of investigation, it does not always correspond to a resistivity contrast. Therefore, an independent map of bedrock elevation was produced using borehole data only. Then this surface was appended to the AEM profiles and used to interpret bounding surfaces that coincide with the bedrock surface. Sedimentary successions were characterized from borehole logs, and AEM data were used to infer the continuity and extent of these sediments.

SEDIMENTARY ARCHITECTURAL UNITS

Large bodies sand and gravel, with subordinate silt and clay, correspond to resistivities >20 ohm-m. Conversely, silt-rich and clay-rich sediments have resistivities <20 ohm-m (Figs 7 to 9, 11 and 12). Examination of AEM profiles revealed several large resistive and conductive bodies that were traceable from profile to profile for several kilometres. The characteristics of these features (linear to slightly sinuous, channel-form geometries) resembled sedimentary bodies, and subsequent targeted borehole drilling successfully verified their existence. Test hole drilling also verified that contacts between major sand and gravel bodies and bodies of silt, clay or diamicton could be mapped using the 20 ohm-m threshold. Detailed comparisons of boreholes and AEM profiles can be found in Divine & Korus (2012) and Korus *et al.* (2013).

Four types of architectural units are identified on the basis of the nature of bounding surfaces (slope, concavity and concordance with land surface), width:depth ratios, and lithology of the fill successions (Figs 5 and 6). These units are described below.

Type I

Bounding surfaces and geometry

Type I architectural units are in the lowermost stratigraphic position, bounded below by the bedrock surface and above by a highly irregular surface representing a composite disconformity at the base of the overlying Quaternary till sheet or channelized deposits (Figs 5 and 7A). The basal surface is a *ca* 12 km wide, west–east trending bedrock depression with sides that slope less than 1°, and it is traceable for more than 150 km (Fig. 1). The basal surface is incised as much as 80 m into underlying substrate, and the width:depth ratio is *ca* 150. The lower and upper surfaces gradually converge towards the edges of the bedrock depression, forming a lenticular sediment body. Type I units are locally absent beneath deeply incised basal surfaces of overlying units (Fig. 5). Where Type II and III units (described below) are absent above a Type I unit, the morphology of the upper surface is generally concordant with the surficial topography some 40 to 50 m above it.

Fill succession

The thickness of the fill succession in the Type I unit varies from 0 to 80 m because of the irregular nature of the bounding surfaces. Although the thickest parts of the fill are most likely to be located near the axis of the west–east bedrock depression, these sediments often thin to zero within a few hundred metres where they are incised by overlying units (Fig. 5). Fill sediments are predominantly fine to coarse pebbly sands and sandy gravels, with a few thin (1 to 3 m) intervals of silt and clay (Fig. 7B). Gravels within this body include clasts of granite, anorthosite and potassium feldspar, and minor amounts of reworked sandstone and limestone. Pink quartzite is notably absent. Gravels are typically found near the base of the succession, but overall there is little to no observable grain-size trend. As such, borehole geophysical logs typically have a cylindrical shape with abrupt lower and upper boundaries. In FDEM profiles, the bulk of the fill succession often lies below the depth of investigation, although the uppermost part is typically resolved as a continuous body of resistivity values between 20 ohm-m and 35 ohm-m (Fig. 5). In TDEM profiles, the entire thickness is within the depth of investigation and appears as a body of high-resistivity values of *ca* 25 to 50 ohm-m directly atop the bedrock surface, which itself corresponds to the *ca* 35 to 40 ohm-m contrast below *ca* 360 m elevation (Fig. 7A).

Type II

Bounding surfaces and geometry

Type II architectural units are comparatively narrow (<1 km), steep-sided (10° to 30° or more) features that underlie small valleys in upland areas (Figs 5, 8A and 8B). These units trend generally north–south, although one trends east–

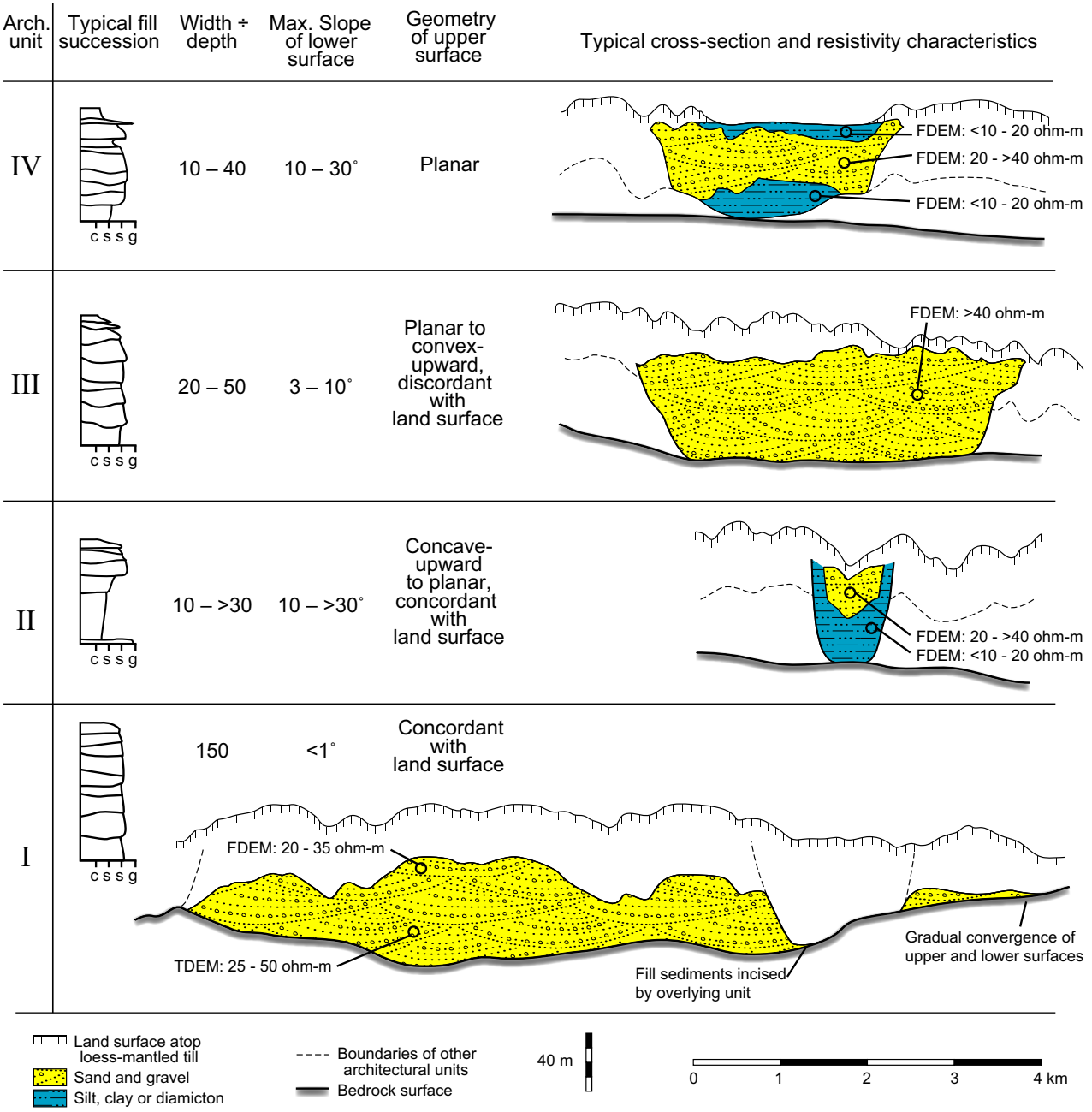

Fig. 5. Principal sedimentary and geophysical characteristics of architectural units. FDEM = frequency-domain electromagnetic; TDEM = time-domain electromagnetic.

west. Type II units are 60 m thick, and their width:depth ratios are 10 to at least 30. Some of these units are fan-shaped in planform, widening from *ca* 1 km to as much as 5 km over a distance of 4 km (Fig. 6). The lower bounding surface is concave-upward and rests on bedrock or on Type I units. The upper bounding surface is broadly concordant with the present land surface and is generally concave-upward, although less so than the basal surface. These units commonly underlie extant stream valleys. Type II units have abrupt terminations along their longitudinal profiles (Fig. 6), and their edges are distinct (Fig. 8A and B).

Fill succession

Sedimentary fills of Type II units are markedly heterogeneous. The lower part comprises 30 to 40 m of silt, clay and diamicton, with thin intervals of sand and gravel (Fig. 8C). Diamicton is

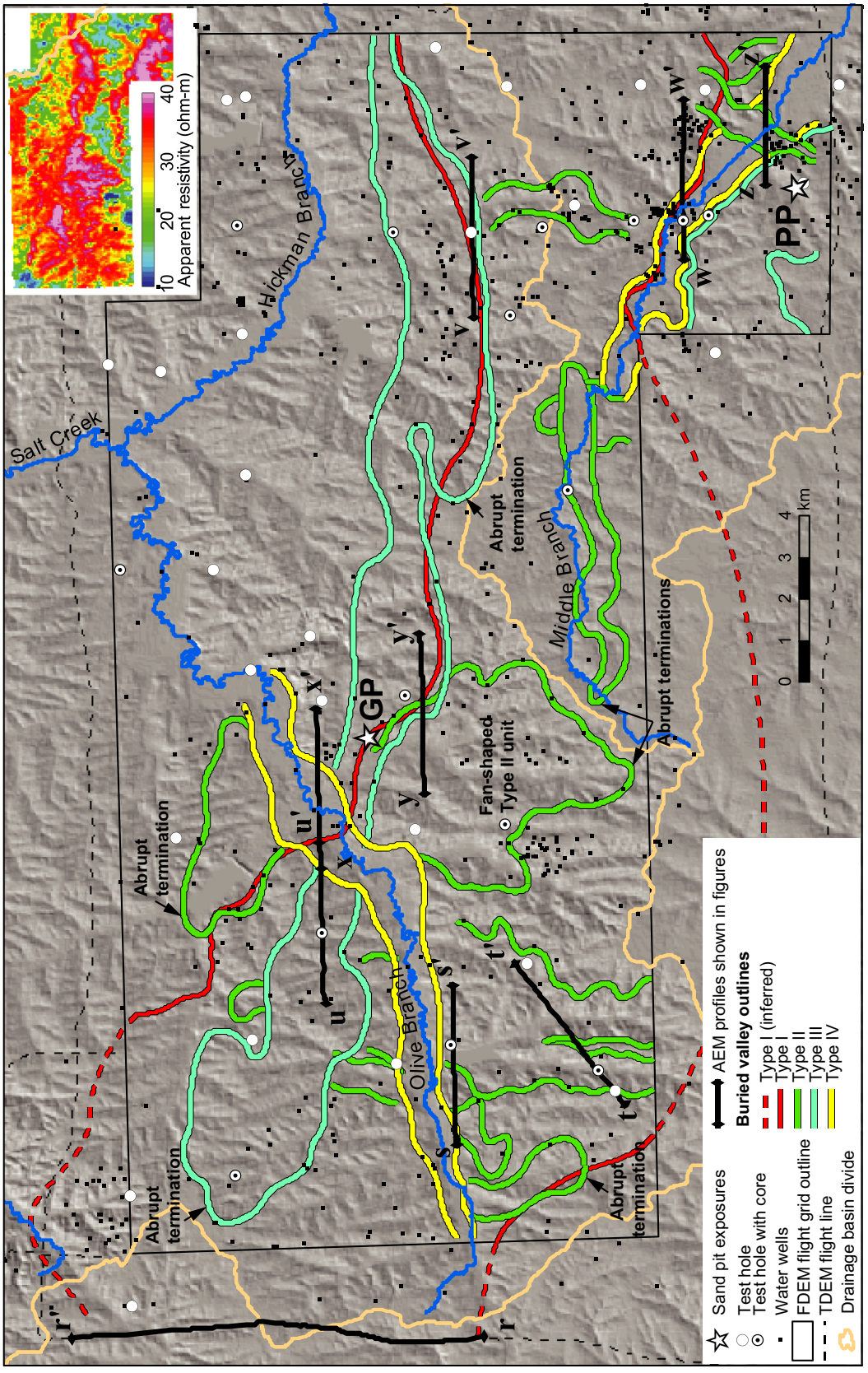

Fig. 6. Map showing boundaries of architectural units and locations of airborne electromagnetic (AEM) profiles, boreholes and sand pits shown in Figs 7 to 12. Inset at upper right shows apparent resistivity (ohm-m) at 8200 kHz, which is sensitive to *ca* 60 m depth. See Fig. 1 for location and regional setting. FDEM = frequency-domain electromagnetic; TDEM = time-domain electromagnetic.

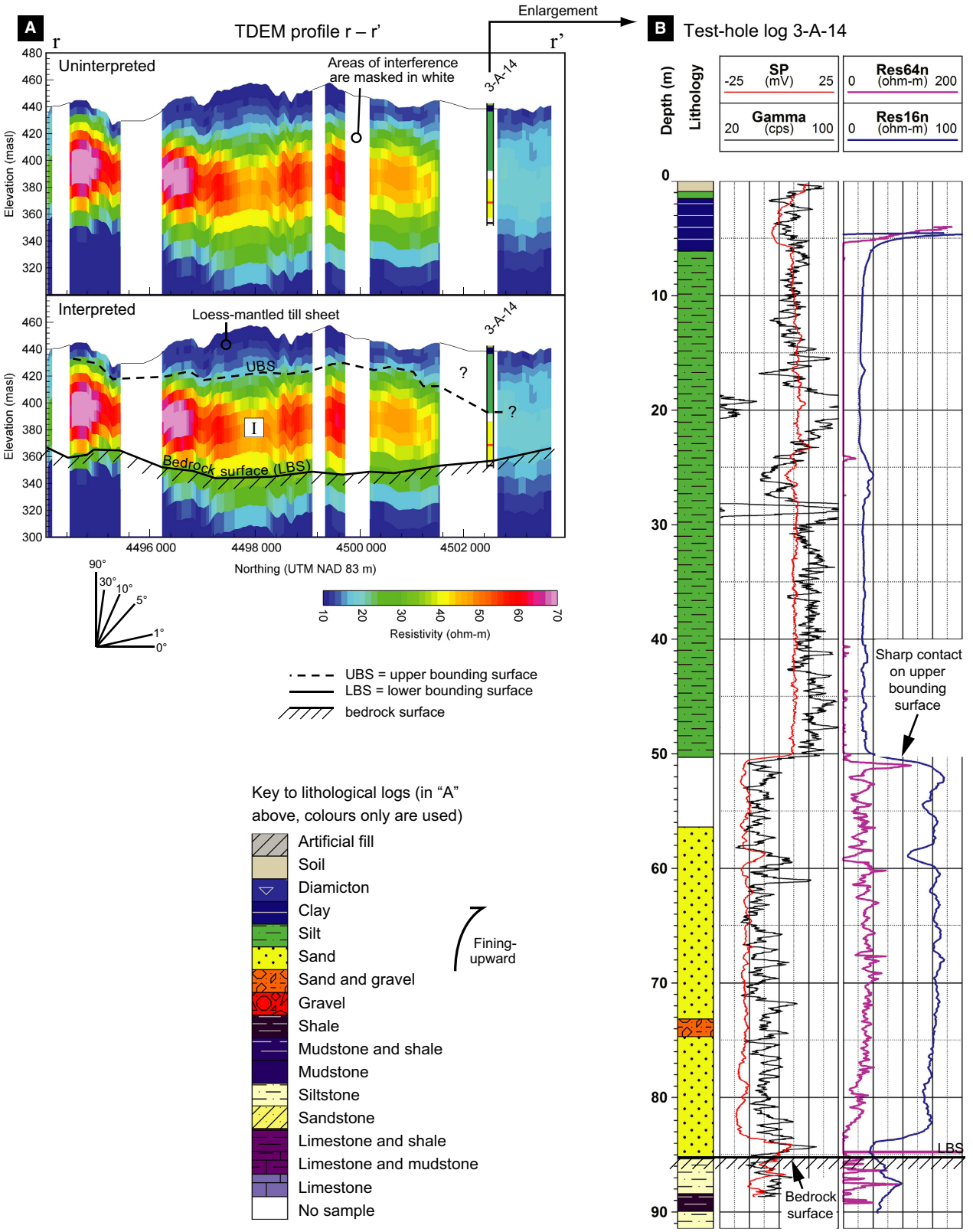

Fig. 7. Example time-domain electromagnetic (TDEM) profile through Type I architectural unit. Geophysical log is from test hole number 3-A-14.

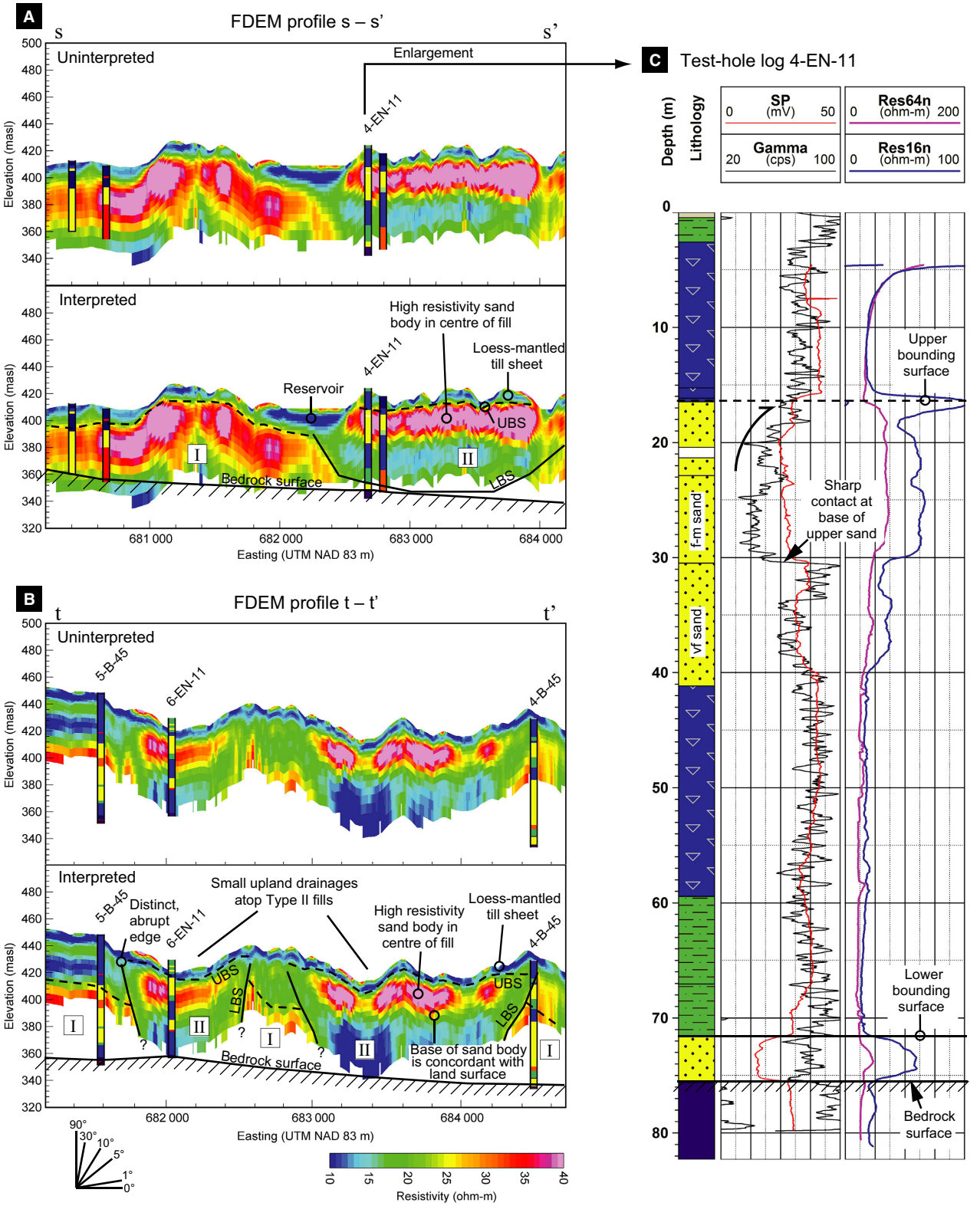

Fig. 8. Example frequency-domain electromagnetic (FDEM) profile through Type II architectural unit. Geophysical log is from test hole number 4-EN-11. See Fig. 7 for legend.

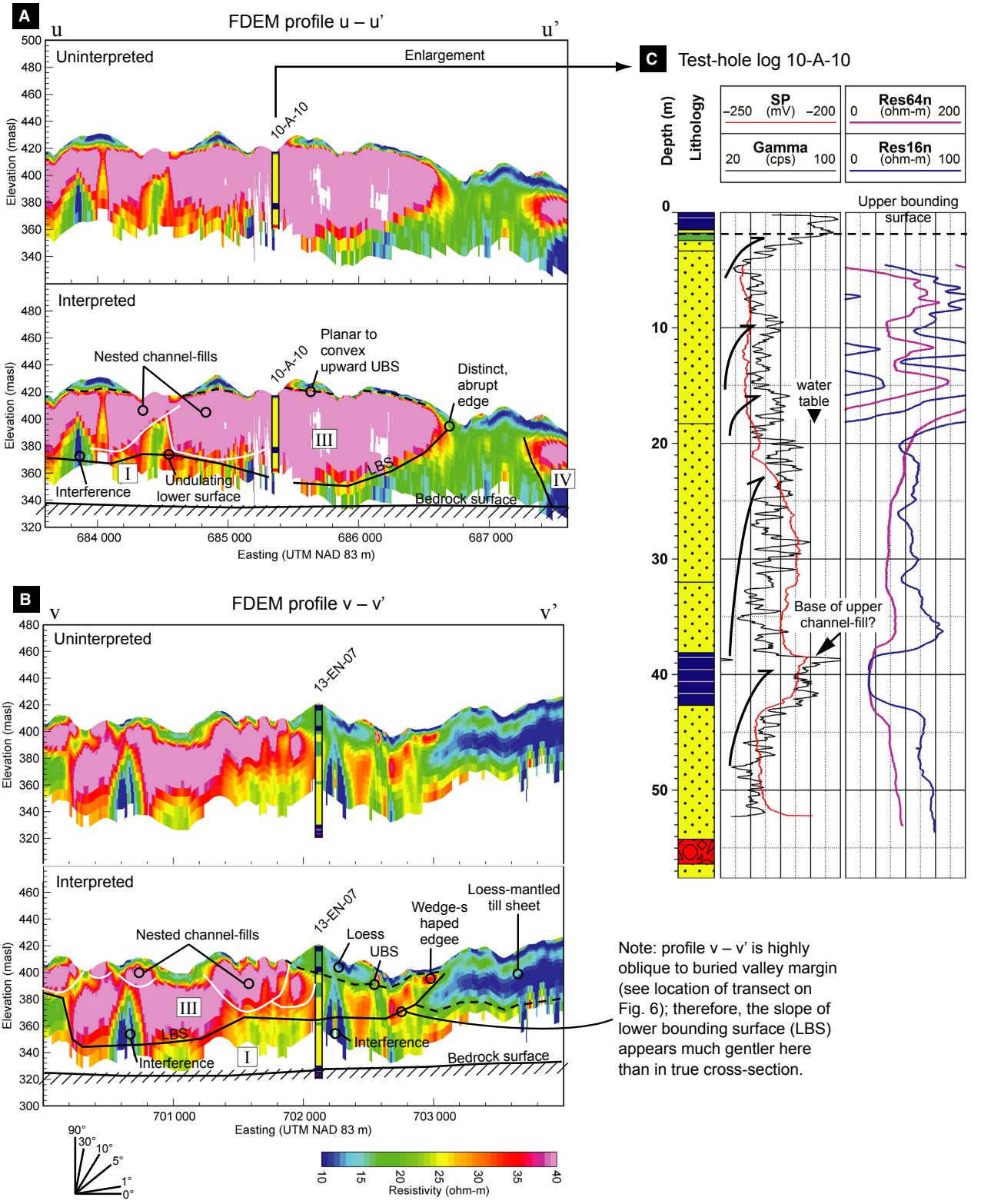

Fig. 9. Example frequency-domain electromagnetic (FDEM) profile through Type III architectural unit. Geophysical log is from test hole number 10-A-10. See Fig. 7 for legend.

present at the bases of some fill successions, directly above the bedrock contact or interbedded with other lithologies in the fill succession. These diamictons are stratigraphically lower than and isolated from the loess-mantled till sheets above the fill successions. The diamictons within the fills are described from test hole cuttings only but, in general, they are dark grey, clay-rich and contain pebbles of limestone, pink quartzite and igneous and metamorphic clasts. The upper parts of the fill succession consist of 20 to 30 m of sand, silty sand and gravel. Gravels include clasts of pink quartzite, limestone and reworked ironstone and sandstone. The fill succession is broadly coarsening-upward, especially near the axis of the unit. In boreholes that penetrate these features, the lithology gradually changes upward from clay, silt or diamicton to silty fine sand to medium-coarse sand, although contacts between units are sharp in some instances. This coarsening-upward sequence is reflected in borehole geophysical logs (Fig. 8C). The AEM signatures of these fill successions are resolvable only in FDEM profiles. Resistivities range from less than 10 ohm-m to greater than 40 ohm-m. The highest resistivity values exist in the upper part of the succession near the centre of the unit. In AEM profiles, they appear as lenticular bodies encased within low-resistivity materials, probably silts, clays and diamictons. Thus, it appears that the sand and gravel bodies within the centres of these fills are gradational into fine sediments or pinch out towards the margins. The upper bounding surfaces of Type II units are succeeded by diamicton, silt or clay.

Type III

Bounding surfaces and geometry

Type III architectural units are recognized as prominent, high-resistivity features, the uppermost parts of which are discordant with the land surface and crop out locally along valley sideslopes (Fig. 9A and B). These features are generally 60 m thick and 1 to 3 km wide, with width: depth ratios ranging from 20 to 50; they are distributed along a broad arc located just north of the divide between two major drainage systems and spanning the entire study area from east to west (Fig. 6). These units are perpendicular to the pattern of small drainages developed on the slopes adjacent to larger stream valleys. The lower bounding surface is generally concave-upward but it is locally undulated and irregular. It rests either directly on bedrock, on deposits of Type I units, or on stratified silts and fine sands above bedrock. The basal surface traces laterally to moderately steep (3 to 10°) margins, which merge with the upper bounding surface within several metres of the land surface. The upper bounding surface is broadly planar to convex-upward, except for where it has been dissected along the modern land surface. Type III architectural units have abrupt terminations spaced 8 to 10 km apart along their longitudinal profiles (Fig. 6). The lateral margins of these units are abrupt to wedge-shaped (Fig. 9A and B).

Fill succession

The fills of Type III units consist of as much as 60 m of sand with lesser amounts of gravel, silt and clay (Fig. 9C). The fill successions comprise nested, high-resistivity sand bodies that are observable in both FDEM profiles and in borehole logs (Fig. 9A to C). Individual sand bodies are *ca* 5 to 15 m in thickness and fine-upward to clay, silt or silty sand. Sand bodies generally thin upward, and they are manifest as multiple, bell-shaped curves in borehole geophysical logs. Gravels contain granite, feldspar, anorthosite, pink quartzite, reworked ironstone and sandstone, limestone and other lithic clasts. Diamicton is thin or absent within these units, except that the entire succession may be capped by diamicton. In some locations the sand body is directly overlain by loess.

Lithofacies in the uppermost parts of Type III fills were examined in two sand pits (Gana and Price pits) located in areas where the resistive bodies in FDEM profile intersect the land surface (Figs 6 and 10). The Gana Pit exposes nearly 20 m of strata dominated by cross-stratified very fine to very coarse sand and pebble gravel with large (as much as 40 cm in diameter) armoured balls of diamicton (Fig. 10A to C). The poorly sorted sands are succeeded by well-sorted sands, overlain by the Gilman Canyon Formation, a pedogenically modified loess deposit, and the Peoria Loess. Although lateral relationships at the scale of the outcrop within the pit could not be examined directly due to excavations, some evidence suggests that the upper parts of the poorly sorted sands may have been laterally equivalent to diamicton (Joeckel & Howard, 2009).

The Price pit exposes mostly medium to very coarse, pebbly sands, with abundant trough cross-bedding (sets as much as 0·75 m thick), ripple trough cross-lamination and horizontal lamination (Fig. 10D). The cross-bedded sands are gradationally overlain by 0·5 to 1·0 m of

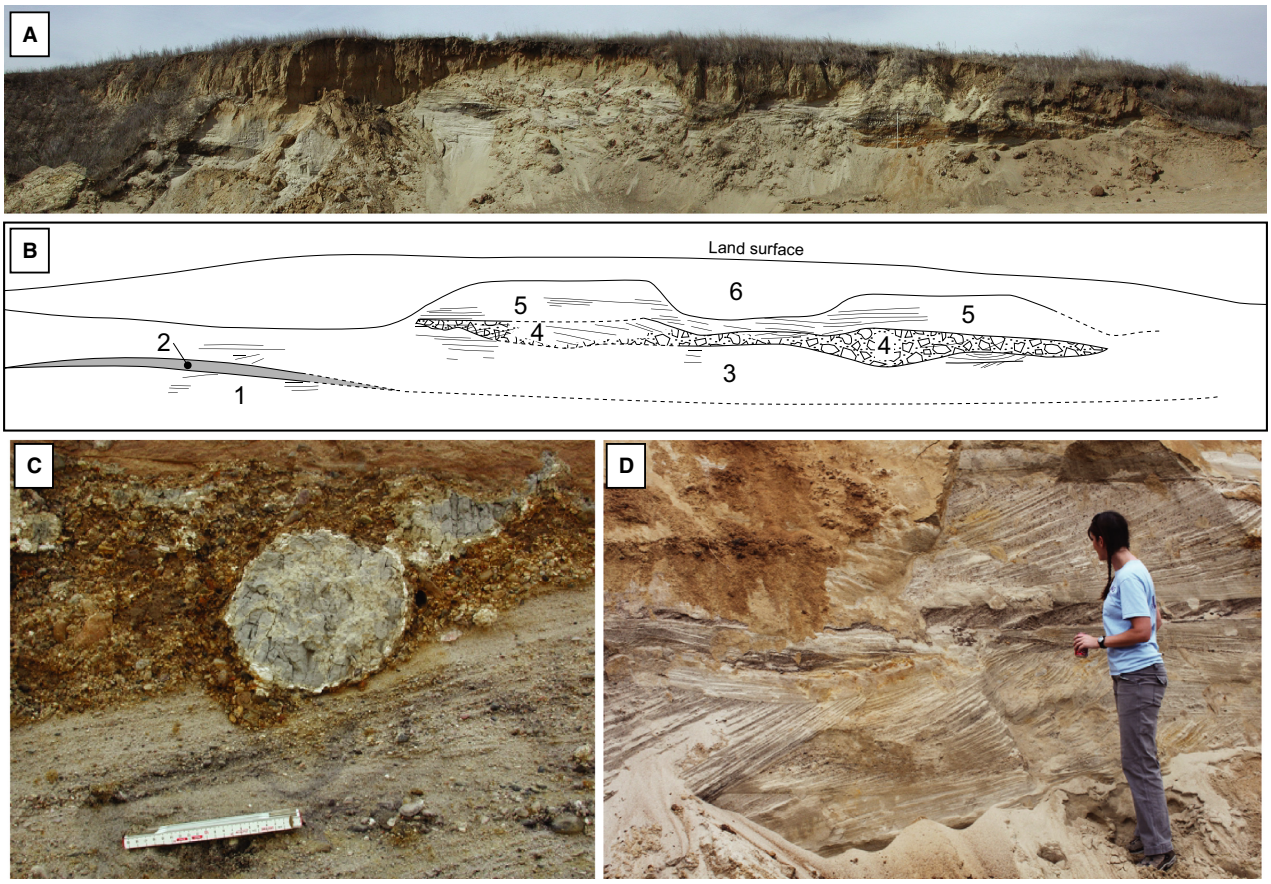

Fig. 10. Photographs of sand and gravel deposits exposed in sand pits. See Fig. 5 for locations of pits. (A) Exposure in Gana Pit (GP). (B) Line drawing interpretation of photograph in (A). Numbers correspond to lithological units: '1' moderately to well-sorted medium sand, few pebbles, trough cross-stratified; '2' massive to faintly rippled silt; '3' well-sorted fine sand, low angle trough cross-stratification, locally horizontal laminae; '4' pebbly sand and pebble to cobble gravel, trough cross-stratified, sets as thick as 100 cm, common, large (as much as 40 cm diameter) armoured till balls; '5' well-sorted fine sand, trough cross-stratified; '6' loess and colluvium. (C) Armoured till balls in unit 4 above. (D) Trough cross-stratified pebbly sands in Price Pit (PP). Person for scale is *ca* 1·8 m tall.

oxidized diamicton, the top of which is the land surface.

Type IV

Bounding surfaces and geometry

Type IV units underlie the valleys of the perennial streams Olive Branch and Middle Branch (Figs 6, 11A and 11B). These units have dimensions similar to those of Type II units: they are narrow (*ca* 1 km), steep-sided (10 to 30°) and *ca* 60 m thick with width:depth ratios of 10 to 40. The lower bounding surface of the unit rests either on bedrock or on deposits of Type I units, although in some FDEM profiles the lack of a clear resistivity contrast precludes the identification of a lower bounding surface. In other profiles, however, clear resistivity contrasts demarcate concave-upward surfaces that abruptly terminate slightly outside the valley margins, under the valley side-slopes. The main difference between Type IV units and Type II units is that the upper bounding surface of a Type IV unit is planar and corresponds to the land surface atop modern alluvium, except under the valley sides where it lies beneath loess-mantled diamicton.

Fill succession

The fills of Type IV units are interpreted mostly from FDEM profiles, although one borehole penetrated such a unit (Fig. 11C). Few boreholes have been drilled into the full thickness of these deposits, so their lithologies are largely unverified. Several profiles exhibit a vertical pattern of resistivity that distinguishes them from laterally juxtaposed units. The resistivity values of Type

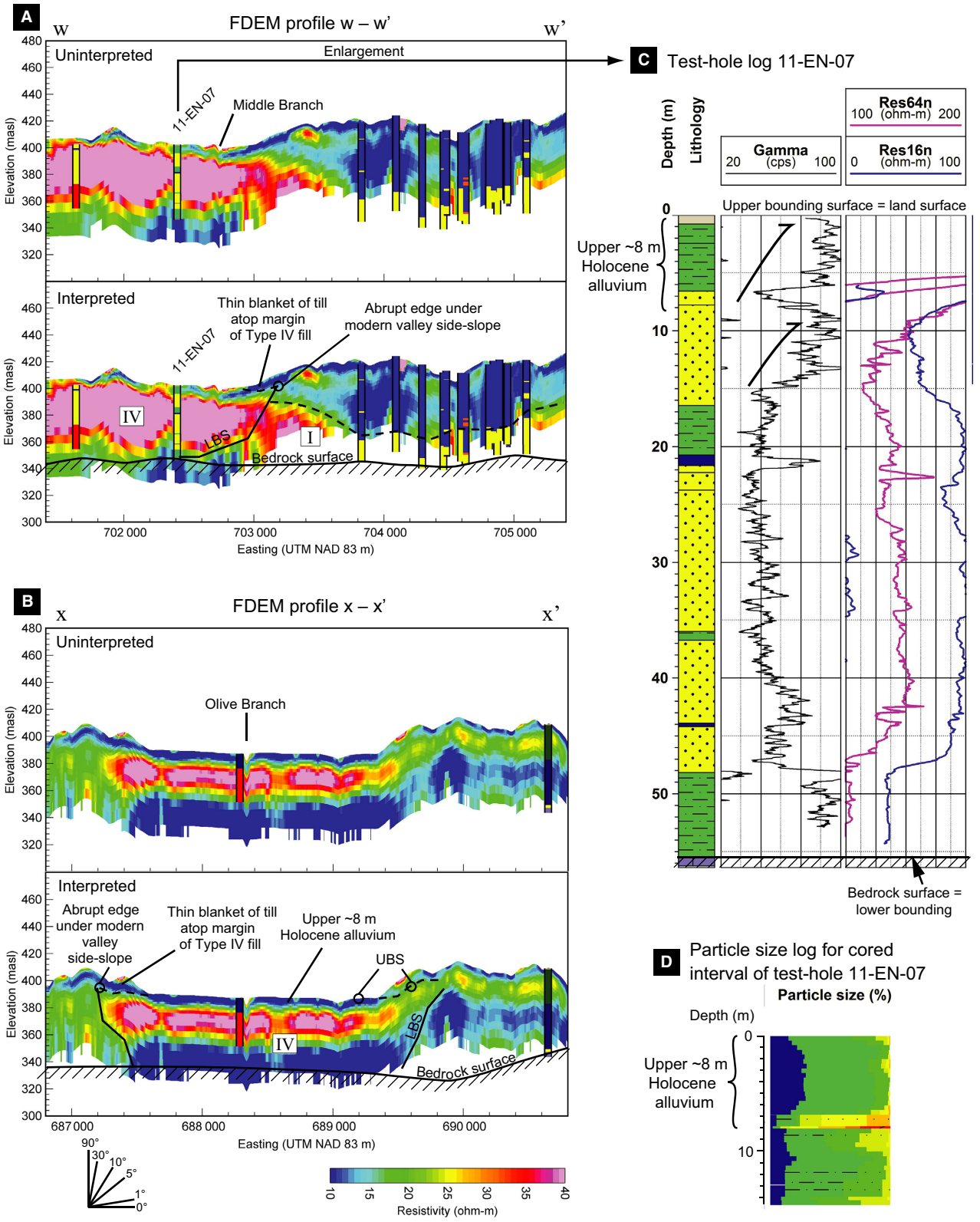

Fig. 11. Example frequency-domain electromagnetic (FDEM) profile through Type IV architectural unit. Geophysical log is from test hole 11-EN-07. See Fig. 7 for legend.

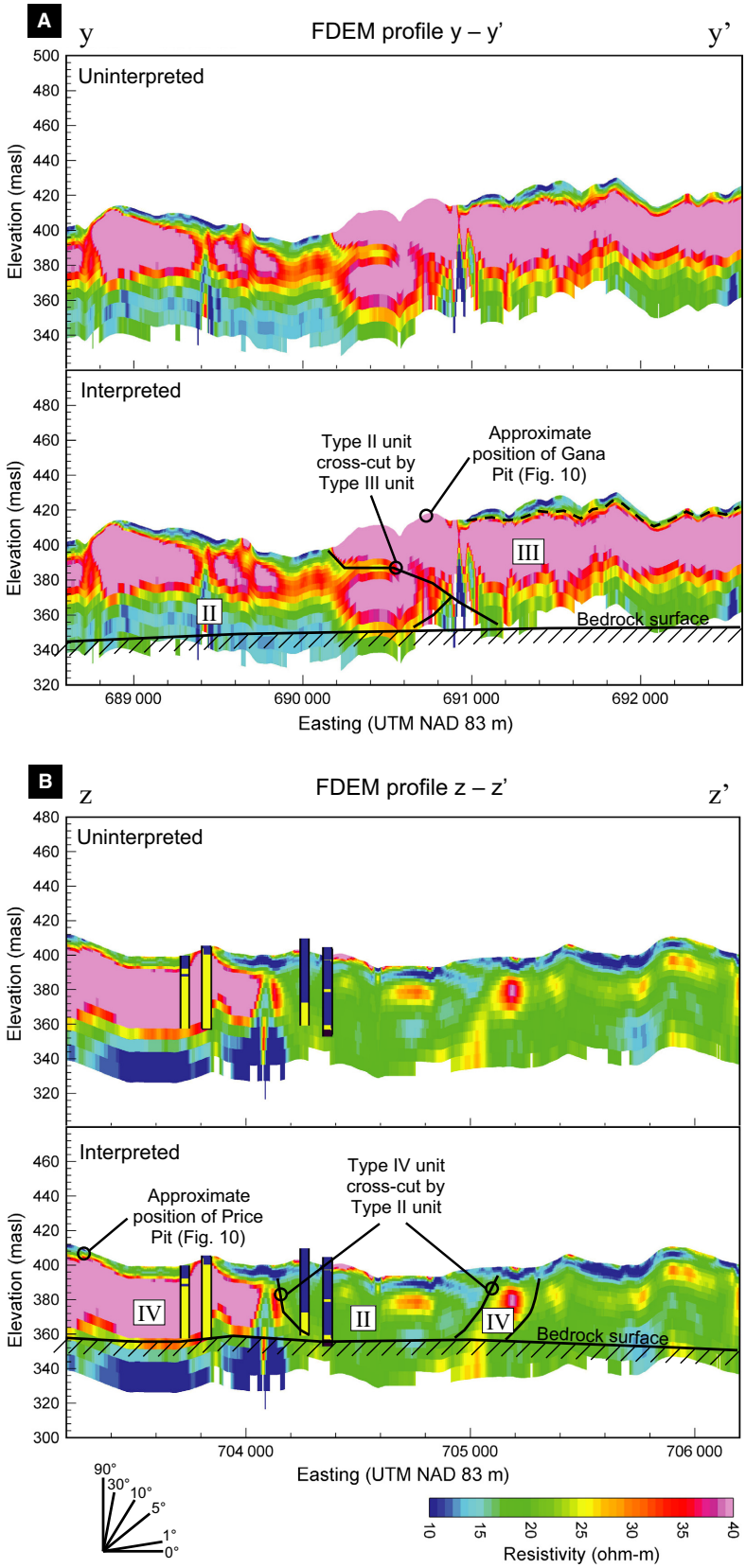

Fig. 12. Example frequency-domain electromagnetic (FDEM) profiles showing examples of cross-cutting relationships. See Fig. 7 for legend.

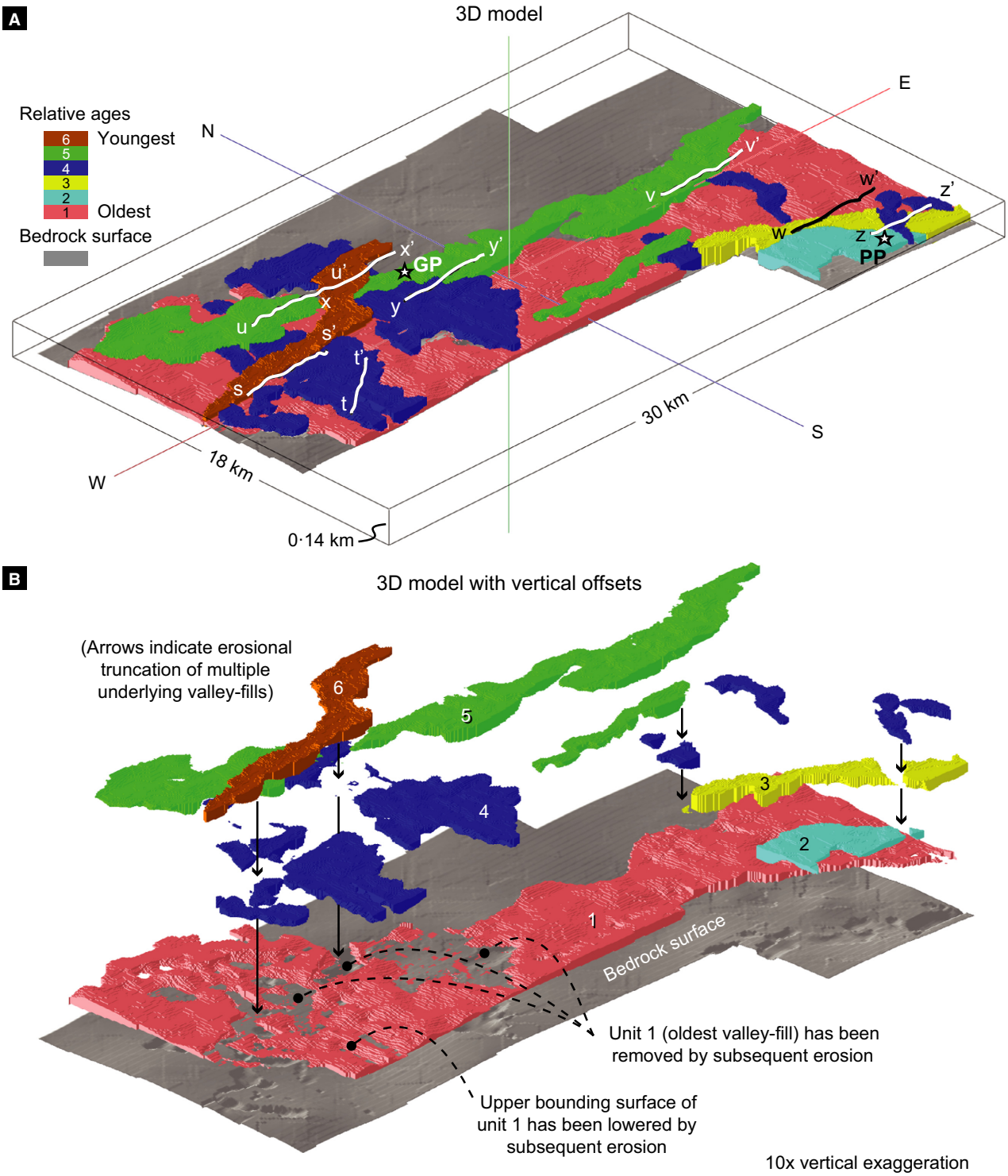

Fig. 13. Three-dimensional geological model of the study area. Bedrock surface modelled from interpretation of borehole data, modified locally using frequency-domain electromagnetic (FDEM) profiles. Buried valleys modelled from interpretation of FDEM profiles and borehole data. (A) Basic 3D model showing locations of profiles shown in Figs 8, 9, 11 and 12, and locations of sand pits shown in Fig. 10. (B) Same as in (A), but with vertical offsets between model layers to illustrate cross-cutting relationships and truncation of older buried valleys beneath younger buried valleys.

IV fills are variable both vertically and laterally. In some places, the lower 10 to 20 m of the unit is low-resistivity material (<10 to 20 ohm-m). In other places, the lower part of the succession is more than 40 m of high-resistivity (20 to >40 ohm-m) material identified in test holes drilled for this study and the logs of previously drilled water wells as sand and gravel. The composition of gravels in these deposits is unknown due to the lack of samples and poor detail in drillers' logs. The uppermost parts of these fills are composed of *ca* 10 m of silty clay and silt to very fine sand, with a thin basal layer of pebbles and cobbles. Resistivity values in these upper units range from less than 10 to 20 ohm-m.

Cross-cutting relationships

Incision and the complex cross-cutting of units are observable in vertical profiles (Figs 8, 9, 11 and 12) as well as in plan view (Fig. 6). The Type I unit is highly discontinuous and variable in thickness because it is partially or completely excised by all overlying architectural units, as observed in several FDEM profiles: s–s′ (Fig. 8A), t–t′ (Fig. 8B), u–u′ (Fig. 9A), v–v′ (Fig. 9B) and w–w′ (Fig. 11A).

Cross-cutting relationships between Types II, III and IV units vary from south to north. In the extreme south-east corner of the study area, a single Type II unit cuts across both Type III and IV units (profile z–z′, Figs 12B and 13). This low-resistivity, fine-grained unit, which has been verified by several driller's logs, infills a deep incision cutting across the otherwise continuous, high resistivity, coarse-grained fill underlying Middle Branch. The modern valley narrows considerably at this location (Fig. 6). The Type II unit is continuous for at least 1 km south-westward into the uplands, where it cuts through the high-resistivity Type III unit before terminating rather abruptly (Fig. 6). Also south of the drainage divide, a single east–west oriented Type II valley cuts across a north–south oriented Type II valley, and a single Type II unit cuts across the drainage divide (Fig. 6).

North of the drainage divide, Type II units are cross-cut by Type III and Type IV units. Cross-cutting is clearly expressed in plan view where north-south trending Type II units intersect the Type III unit trending west–east across the study area (Fig. 6). This relationship is also shown in profile y–y′ (Fig. 12A). Type III units north of the divide are cross-cut only by Type IV units, and the Type IV unit underlying Olive Branch is not cross-cut by other features.

INTERPRETATION

Type I units: palaeovalley fills

The bedrock depression associated with Type I units has long been regarded as part of a large network of pre-Pleistocene bedrock palaeovalleys which were later overridden by glacial advances (Lugn, 1935; Reed & Dreeszen, 1965; Dreeszen & Burchett, 1971). Indeed, these features display many characteristics consistent with that interpretation. The width:depth ratio of *ca* 150 is within the wide range of dimensions of bedrock palaeovalleys worldwide (Gibling, 2006), but it is considerably higher than those of subglacial tunnel valleys (*ca* 10; Barker & Harker, 1984; Gibling, 2006; Ahmad *et al.*, 2009; van der Vegt *et al.*, 2012). The valley dimensions, its west–east course through the region, and the slope of its margins (<1°) all argue against a subglacial drainage origin.

There has been less agreement, however, regarding the genesis of the sedimentary fill within the palaeovalley. The palaeovalley fill may be preglacial (deposited before *ca* 2·6 Ma), synglacial (deposited at the time of a glacial stage earlier than the one during which the overlying till was deposited) or interglacial (deposited between glacial advances that occurred prior to *ca* 640 ka), or some combination thereof. Most previous interpretations focused on a synglacial origin. Reed & Dreeszen (1965) interpreted the fills as proglacial deposits formed ahead of an advancing Laurentide Ice Sheet. Emery (1966), Keech *et al.* (1967) and Ginsberg (1983) interpreted them as the fills of drainageways blocked by synglacial ice. The continuation of west–east trending buried valleys across the westernmost limit of the Laurentide Ice Sheet, however, suggests that they are either preglacial or interglacial. Moreover, there is no physical evidence that these streams were deflected southward along an ice margin.

The gravel composition (granite, anorthosite, feldspar, without pink quartzite) can be used in a general sense to distinguish these gravels from gravels within overlying Type II and Type III architectural units. This composition indicates a Rocky Mountain provenance, rather than an affiliation with glacial detritus derived from the

Canadian Shield and Sioux Quartzite ridge to the north and north-east of Nebraska (Stanley & Wayne, 1972). The absence of reworked glacial-erratics renders a synglacial origin of the palaeovalley fill highly unlikely. Definitive evidence for the interglacial hypothesis is also lacking, although the logs of a few test holes drilled in the 1940s describe 'till' beneath palaeovalley fill sediments and above the bedrock surface. It can be difficult to identify till in rotary cuttings, however, and many of these early interpretations are considered questionable. Furthermore, none of the test holes drilled for this project encountered till in this stratigraphic position.

The upper bounding surface is a composite surface which has been greatly modified by erosion beneath younger deposits. Incisions of 40 to 50 m on the upper surface correspond to the locations of overlying channelized deposits (Figs 7A, 7B, 8B, 10A and 13). The incisions commonly penetrate to bedrock, completely truncating the Type I fill.

Type II units: under-filled tunnel valleys

Type II units are classified as Quaternary sediment buried valleys (Russell *et al.*, 2004). These buried valleys have several characteristics that are inconsistent with a non-glacial fluvial origin; they are steep-sided (10 to 30° or more), have width:depth ratios from 10 to more than 30, and terminate abruptly, although they are emplaced in erodible sediments (van der Vegt *et al.*, 2012). Terminations tend to coincide with the drainage divide interpreted by others as a regional, moraine-controlled topographic feature (Reed & Dreeszen, 1965). Huuse & Lykke-Andersen (2000) and van der Vegt *et al.* (2012) consider abrupt beginnings and endings with undulating long profiles and large overdeepenings among the diagnostic criteria to distinguish tunnel valleys from non-glacial fluvial valleys. Indeed, the dimensions, U-shaped morphology and infill successions of these architectural units are in excellent agreement with other well-documented tunnel valleys worldwide (e.g. Piotrowski, 1994; Fisher *et al.*, 2005; Jørgensen & Sandersen, 2006; Kristensen *et al.*, 2007; Pugin *et al.*, 2014).

The sedimentary succession can be subdivided into two distinct parts: a lower part containing silt, clay and diamicton, and an upper part containing predominantly sand. The silts and clays are interpreted as glaciolacustrine deposits, whereas diamicton could have formed by ice creep and collapse into the valley, forming a till unit, or from debris flows into a meltwater-filled valley. The two possible geneses hold significant implications as to the timing and development of the valleys during glaciation, but the lack of surface exposures and cores of valley-fill diamicton precludes a more detailed assessment of the depositional environment. The final stage of infilling is represented by channel sands near the top of the fill. Most of these sand bodies have channel-form geometries interpreted from AEM profiles and are contained wholly within the fine-grained fill. Sands contain gravel clasts of Sioux quartzite, metamorphics and reworked bedrock, indicating a glacial origin. This multi-stage fill succession resembles tunnel-valley fills described by Piotrowski (1999), Jørgensen & Sandersen (2006) and Kehew *et al.* (2013).

Type II tunnel valleys underlie small drainageways, although some modern drainages do not overlie interpretive tunnel valleys. The upper bounding surfaces were modified by incision of interpretive, cross-cutting tunnel valleys and by interglacial and post-glacial erosion and deposition in the drainages. The lower surfaces of sand bodies within the fills commonly mirror the land surface above (Fig. 8B), suggesting that the modern topography is at least partially inherited from the original tunnel-valley morphology. This palimpsest drainage pattern could relate to the erosion of less resistant sand or it may reflect drainage development over pre-existing topographic lows. Regardless of the formative process, the Type II tunnel valleys are expressed at the land surface, their upper bounding surfaces are concave-upward, and they are incompletely filled with sediment (cf. Fisher *et al.*, 2005). The thin diamicton drapes atop the tunnel valleys are generally concordant with the upper and lower surfaces of the sand bodies within the fill, as well as with the surface topography. The overlying diamicton was either emplaced during melt-out as debris and ice collapsed into the valley (e.g. Kehew *et al.*, 2013) or during a later glacial advance (e.g. Piotrowski, 1994).

Type III units: over-filled tunnel valleys

Type III units share many characteristics with Type II units, except that the upper surface of the former is generally planar to slightly convex-upward and is discordant with the land surface. It has been suggested, on the basis of limited data from a few exposures (Fig. 10), that outcropping sand bodies in the study area may

be glacial outwash (Joeckel & Howard, 2009). In light of the new information presented herein, it is suggested that the outcropping sediments represent the uppermost parts of thick (up to 60 m) valley-fill successions extending downward to the bedrock surface. Significant erosion of the substrate is difficult to explain in an outwash hypothesis, because fluvial outwash systems tend to occupy broad, unconfined, aggradational plains and alluvial fans (Smith, 1985; Fisher *et al.*, 2005; Marren *et al.*, 2009). Although the outwash hypothesis cannot be refuted altogether, it is posited that the basal erosion surfaces of Type III units originated as tunnel valleys because they exhibit deep incisions with steep sides (3 to 10°), they have undulating long profiles and overdeepenings, and they terminate abruptly along their long profiles, commonly at interpretive moraines. Their fill successions are complex, however, and they are filled not only with tunnel valley sediments, but with a significant proportion (50% or more) of outwash sediments.

The fill successions of Type III units are compound, consisting of multiple, nested channel fills representing multiple reoccupations of the tunnel valleys (Fig. 9). These channel fills are the deposits of streams draining from the terminus of the retreating Laurentide Ice Sheet. The existence of an aggrading outwash system atop the Type III fill would, in effect, explain the planar to convex-upward geometry of the upper surface (e.g. Kjær *et al.*, 2004). It is reasonable to assume that the valleys would have been reoccupied by ice-contact, melt-water streams upon glacial retreat, since streams are often sequestered along the ice margin due to overdeepening (e.g. Marren *et al.*, 2009) and moraine-confinement (e.g. Russell *et al.*, 2006). Moreover, reoccupation of previously formed tunnel valleys has been documented elsewhere (Jørgensen & Sandersen, 2006). The upper part of the fill succession is highly dissected and is exposed locally at the land surface. In some areas the valley margins closely coincide with divides between higher-order, upland drainages, suggesting that the sediment body may have originally had positive topographic relief (Fig. 6). On the basis of the geometry of the upper bounding surface and the topographic expression, it is suggested that the Type III tunnel valleys were 'over-filled', i.e. the confined tunnel valleys were converted to unconfined outwash fans/aprons as the glacier retreated from the area. The original depositional topography was later eroded.

Type IV units: under-filled tunnel valleys, reoccupied by modern streams

Type IV units are similar to Type II and Type III units. They are deep, steep-sided, U-shaped incisions that, in some cases, clearly penetrate to bedrock. The uppermost 8 m of sediment in test hole 11-EN-07 is interpreted as Holocene alluvium (Fig. 11). Grain-size analysis of these near-surface deposits shows a thin gravel lag fining-upward into sand and then silt, consistent with an alluvial origin from a small, meandering stream. The uppermost *ca* 8 m of Type IV units elsewhere are expressed as low-resistivity sheets atop thick (30 to 50 m), high-resistivity bodies of sand and pebbly sand. It is unlikely that the thick successions of coarse-grained sediment are wholly the result of alluvial processes associated with the modern streams under which they lie. The 60 m thick succession, for example, lies merely 6 km downstream of the headwaters of Middle Branch, and it is truncated by a Type II unit just 4 km upstream of the location of the profile (Figs 6 and 11). The modern catchment area upstream the terminus of the tunnel valley-fill is a mere 30 km^2. Fluvial-channel scour of 60 m is possible only in the largest river systems on Earth (e.g. Best & Ashworth, 1997; Fielding, 2007). It is therefore necessary to invoke glacial meltwater as the cause of the incision, because the energy required to scour to these depths could have easily been supplied by catastrophic release of subglacial lake water or gradual melting of stagnant ice (Fisher & Taylor, 2002; Hooke & Jennings, 2006; Sandersen *et al.*, 2009; Kehew *et al.*, 2012).

The margins of Type IV units extend slightly under the valley side-slopes (Figs 6 and 11), which consist of loess-mantled till less than 10 m in thickness (Joeckel & Dillon, 2007a,b; Joeckel & Howard, 2009). The presence of till above the fill sediments indicates that Type IV tunnel valleys formed before or during deglaciation in the area. These units are expressed as negative topographic relief, just as are Type II units, which are interpreted as the fills of tunnel valleys. Thus, Type IV units are interpreted as under-filled tunnel valleys that were later reoccupied by modern streams. Nevertheless, the fills underlying Middle Branch and Olive Branch are likely to be of different ages.

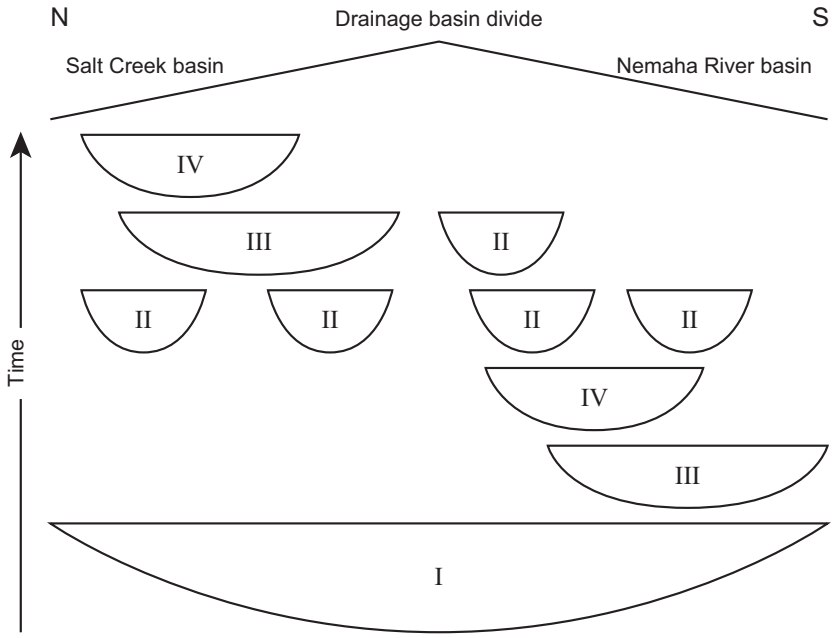

Fig. 14. Postulated evolution of buried valley networks in the study area, on the basis of relative ages and location relative to drainage basin divide. The precise relationship between Type II tunnel valleys north versus south of the divide cannot be determined from cross-cutting relationships, and therefore they are inferred to be of the same generation on basis of north–south orientation and similar sedimentary architecture. Not to scale relative to time, thickness or distance.

DISCUSSION

Ages and stratigraphic relationships of units

Age dates for Pleistocene sediments in the study area are very limited. Optically stimulated luminescence ages are reported in Joeckel & Howard (2009) for the Gana Pit (Fig. 10), which exposes the uppermost *ca* 20 m of a Type III tunnel valley-fill. Alluvial sediments at the top of the fill succession yielded ages in excess of 100 ka. However, wind-reworked sands atop these sediments yielded an age of 53·2 ± 4·3 ka, and two optical ages for the overlying Gilman Canyon Formation were reported as 33·9 ± 2·7 and 34·6 ± 3·0 ka.

Cross-cutting relationships indicate a complex, multi-phase history of buried valley formation in the study area (Fig. 14). The palaeovalley fill is the oldest unit of all, because it is bounded at the base by the bedrock surface and at the top by a composite disconformity formed on the bases of all overlying units. The interpretive tunnel valleys within glacial sediments are more complex, and their relative ages vary from south to north across the drainage divide between the Salt Creek and the Nemaha River catchments (Figs 6 and 14). South of the drainage divide, the Type III unit (Fig. 6) is the oldest tunnel valley, followed by the Type IV tunnel valley underlying Middle Branch. These tunnel valleys were succeeded by two generations of Type II valleys. North of the divide, Type II tunnel valleys are the oldest features since they are cut by east–west trending Type III and IV tunnel valleys (profile y–y′, Fig. 11). The long, east–west trending Type III valley represents the next generation. The youngest tunnel valley underlies Olive Branch (Fig. 6).

No tunnel valley intersects all Type III and IV units on either side of the divide, so direct comparison of relative ages is not possible. The most parsimonious explanation, however, is that all north–south oriented Type II units represent a single generation of buried valleys, since they share similar geometries, orientations and stratigraphic successions. Indeed, other studies have shown that generations of tunnel valleys can be inferred from orientation and associated stratigraphic features (Fisher *et al.*, 2005; Kristensen *et al.*, 2007; Høyer *et al.*, 2015). It is therefore postulated that the Type III and IV tunnel valleys south of the Salt Creek–Nemaha River drainage divide are older than the Type III and Type IV valleys north of the divide (Fig. 14).

On the basis of these relative ages, there must be at least six generations of buried valleys represented in the study area, including the progenitor bedrock-interface palaeovalley that predates the formation of the tunnel valleys (Fig. 14). Tunnel valleys are interpreted to become progressively younger northward, which is consistent with the direction of glacial retreat in the

region. The drainage divide separates different generations of time-transgressive tunnel valleys, and in most cases these valleys terminate abruptly at the divide (Fig. 6). These relationships support the idea that the divide is indeed the topographic expression of an important glacial landform, such as the remnant of a recessional moraine (Lugn, 1935; Reed & Dreeszen, 1965).

Tunnel-valley infill

The geometry, fill succession, and negative topographic expression of the under-filled Type II and Type IV tunnel valleys resemble the 'open tunnel valleys' of Denmark (Jørgensen & Sandersen, 2006) and 'incompletely filled' tunnel valleys of Michigan, USA (Fisher *et al.*, 2005). Incomplete filling of tunnel valleys has been documented in the North Sea basin as well (Bradwell *et al.*, 2008). In some cases the post-glacial infill may be an important part of the infill succession of incompletely filled tunnel valleys (van der Vegt *et al.*, 2012). In the present study, however, although the tunnel valleys are incompletely filled, they are partly to completely buried by sheets of till and loess-mantled till (s–s′ and t–t′, Fig. 8; w–w′ and x–x′, Fig. 11). The post-glacial infill is therefore only a minor part of these successions.

The infill of tunnel valleys varies greatly depending on the dynamics of the ice sheet under which they form. Fine sediments and diamicton are often interpreted as having been deposited distal to the ice margin, whereas coarse sediments are deposited in proximal settings (e.g. van der Vegt *et al.*, 2012; Janszen *et al.*, 2013). Van der Vegt *et al.* (2012) argue that infill successions formed during ice advance should contain a large proportion of subglacial tills and lacustrine deposits. The under-filled tunnel valleys in the present study exhibit distinct fill successions comprising fine-grained sediments at the base and coarse-grained sediments at the top. Silty sediments at the bases of the fills are of likely glaciolacustrine origin and probably were deposited beneath the ice, because they occupy the deepest parts of the tunnel valleys and are conformably overlain by ice-derived diamicton. This interpretation implies that subglacial meltwater was impounded and trapped under the ice following formation of the valley. The termini of most of these tunnel valleys correspond to the

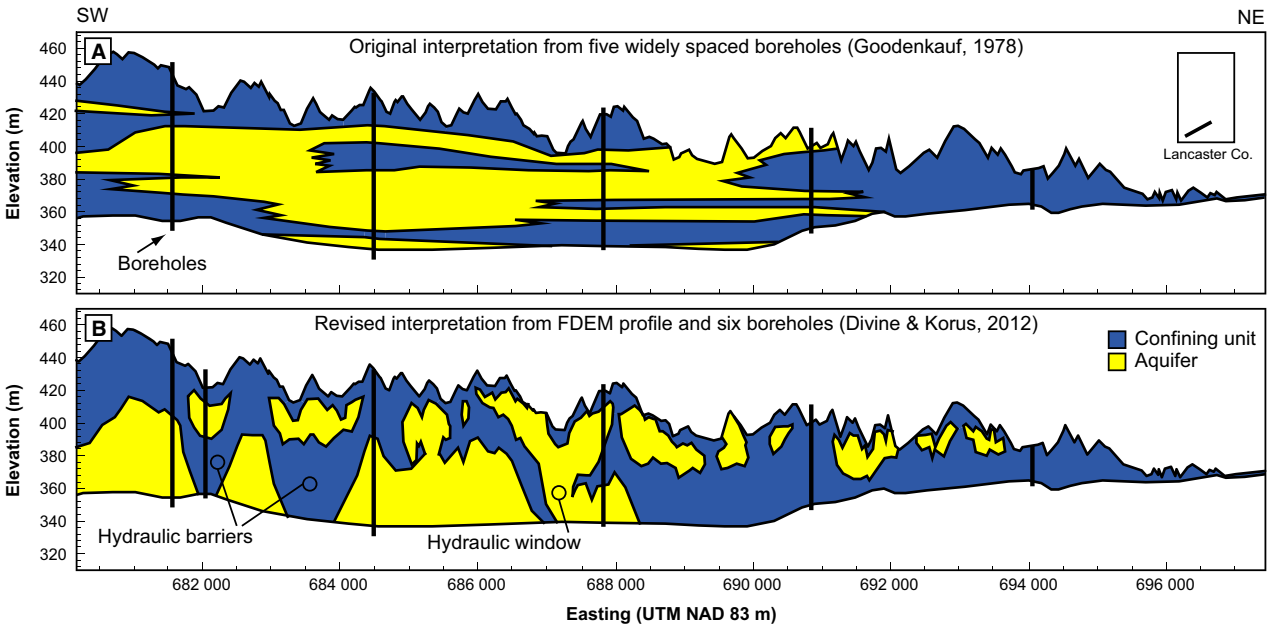

Fig. 15. Comparison of two hydrostratigraphic interpretations of same south-west to north-east transect through the study area. (A) Original interpretation by Goodenkauf (1978) from correlation of stratigraphic units between five widely spaced boreholes. (B) Revised interpretation by Divine & Korus (2012) from correlation of high-resistivity bodies in frequency-domain electromagnetic (FDEM) profile, aided by data from the same five boreholes plus one additional borehole drilled as part of this study. Minor differences between interpretations in the vicinity of boreholes reflect lateral variability between offset borehole and profile locations. Also, some thin sand bodies encountered in boreholes do not appear in revised correlation because they do not correspond to continuous features in FDEM profiles, and therefore have little hydrostratigraphic significance.

previously interpreted moraine (Lugn, 1935; Reed & Dreeszen, 1965), as opposed to outwash fans indicative of rapid release of meltwater during outburst events (e.g. Cutler *et al.*, 2002; Hooke & Jennings, 2006). It appears, therefore, that these tunnel valleys were filled, in part, under conditions of low-energy and comparatively limited sediment supply.

The over-filled Type III tunnel valleys, on the other hand, contain little or no fine sediments or diamicton indicative of stagnant meltwater and they are not preserved as negative topographic relief. The coarse-grained nature of the infill and the presence of outwash sediments suggest deposition in proximity to the ice margin where meltwater and sediment were abundant.

On the basis of this limited evidence, it is speculated that deposition within under-filled tunnel valleys happened during ice sheet advance or stagnation, whereas over-filled tunnel valleys filled during ice retreat. Testing of these hypotheses may require more detailed sedimentological data, expansion of the study area to include a broader spectrum of deposits downstream of tunnel-valley termini and comparisons with tunnel valleys elsewhere along the glacial margin.

Hydrostratigraphy

A hydrostratigraphic unit is a body of sediment or rock with distinct hydrological properties, such as type of porosity or a characteristic range of hydraulic conductivity (Maxey, 1964; Seaber, 1988). Buried valleys are often conceptualized as confined aquifer systems because they are commonly covered by impermeable sheets of till (e.g. Cummings *et al.*, 2012). In the present study, the existence of Type III over-filled tunnel valleys atop a deeper, bedrock-interface valley, provides highly localized hydrological 'windows' in which the aquifer is locally unconfined and vertically connected as a single aquifer body (Fig. 15B). These windows are sites of focused recharge and are susceptible to contamination from non-point agricultural sources (Divine & Korus, 2012; Korus *et al.*, 2013). Hydraulic barriers, which prevent the flow of groundwater between aquifers, can also be identified. Hydraulic barriers exist where Type II tunnel valleys excise the underlying aquifer materials of the Type I buried valley (Fig. 15B). Another barrier, similar to those documented by Shaver & Pusc (1992) in North Dakota, USA, is present under Middle Branch (Figs 6 and 12B). The mechanisms controlling the formation and infilling of the tunnel valleys clearly relates to the complex hydrostratigraphic framework. Knowledge of the sedimentary geology of these deposits is therefore of critical importance for understanding the physical hydrology of the groundwater system and its connection to surface water. The categorization of aquifers in this manner has important implications for groundwater management, because depletions to stream flows and groundwater storage due to pumping are closely related to aquifer continuity, degree of confinement and stream-aquifer interconnectivity (Lohman, 1972; Balleau & Mayer, 1988; Korus & Burbach, 2009).

In this study, 3D analysis of hydrostratigraphic units was possible only by integrating closely spaced frequency-domain electromagnetic (FDEM) resistivity profiles with a wealth of borehole data. Lessons learnt in this study suggest that grid spacing, vertical resolution and depth of investigation are among the most important considerations. In areas of thick, clay-rich till, the depth of investigation of FDEM may be severely limited. The depth of investigation of the FDEM in this study was *ca* 50 to 80 m, which was insufficient to map the full thickness of Quaternary sediment. The time-domain electromagnetic (TDEM) profile, which was used in this study on a very limited basis, provided a much greater depth of investigation sufficient to penetrate bedrock. However, the vertical resolution of TDEM was much lower than that of FDEM. Whereas TDEM was useful for mapping the bedrock surface and the sedimentary fill of the large, bedrock-interface valley in the deep subsurface, the finer details of the tunnel valleys could only be mapped using FDEM.

CONCLUSIONS

Buried valleys are common features of glaciated landscapes, but their complexity makes characterizing the sedimentary architecture and hydrostratigraphy of these deposits particularly challenging. This study demonstrates that airborne electromagnetics (AEM) can be used effectively in settings with a high degree of lithological heterogeneity to identify sedimentary architectural units tens of metres in depth and ranging from 100 m to more than 1000 m in width. In such settings, airborne electromagnetics offers a distinct advantage over other techniques: employment of airborne electromagnetics permits rapid surveying of large areas for comparatively low cost (Robinson *et al.*, 2008). Geophysical

inversion is an important part of the interpretation, because it allows for detailed three-dimensional analysis and identification of features that cannot be resolved in two-dimensional maps or profiles alone.

At least six generations of buried valleys are represented in the study area, indicating a complex, multi-phase history of glaciation and buried valley genesis. A bedrock-interface palaeovalley preceded the formation of a complex network of tunnel valleys. The oldest tunnel valleys are located south of a moraine-controlled drainage divide and are oriented east–west. Intermediate-age tunnel valleys are oriented north–south and are located on both sides of the divide. These valleys are cross-cut by a younger set of east–west tunnel valleys. The youngest tunnel valley is located north of the divide and underlies a modern stream valley. The progressive shift northward of tunnel valleys through time is consistent with the direction of glacial retreat in the region and is also consistent with the interpretation of the drainage divide as a recessional moraine. The recognition of different fill successions indicative of variable energy and sediment supply regimes and of depositional topography in these highly dissected landscapes contributes to a broader understanding of the complex glacial–deglacial history of pre-Illinoian glaciations in the North American interior.

This study provides a significant advancement in the understanding of hydrostratigraphy in pre-Illinoian glacial deposits of North America. The seemingly random occurrence of inter-till aquifers in geological settings such as this one can now be assessed in terms of a tunnel-valley hypothesis, and the orientation, geometry and continuity of such units can be tested against this model. The recognition of under-filled tunnel valleys with fine-grained fills beneath higher-order streams and drainages suggests that depositional topography is at least partially preserved in this dissected landscape, and such topography relates directly to the potential existence of hydraulic barriers within the aquifer system. This finding has important implications for exploring and managing groundwater resources in similar geological settings elsewhere.

ACKNOWLEDGEMENTS

Funding was provided by Nebraska's Natural Resources Districts (NRDs), the Nebraska Department of Natural Resources, the Nebraska Environmental Trust, and the US Geological Survey. Special thanks to Katie Cameron, coordinator of the Eastern Nebraska Water Resources Assessment (ENWRA), Les Howard, cartographer, and Matt Marxsen, field services coordinator, School of Natural Resources, University of Nebraska-Lincoln. We gratefully acknowledge Riley Mulligan and an anonymous reviewer for their thoughtful and careful reviews.

REFERENCES

Abraham, J.D., **Bedrosian, P.A.**, **Asch, T.H.**, **Ball, L.B.**, **Cannia, J.C.**, **Philips, J.D.** and **Lackey, S.O**. (2011) Evaluation of geophysical techniques for the detection of paleochannels in the Oakland Area of Eastern Nebraska as Part of the Eastern Nebraska Water Resource Assessment, U.S. Geological Survey Scientific Investigations Report 2011-5228, 40 pp.

Ahmad, J., **Schmitt, D.R.**, **Rokosh, C.D.** and **Pawlowicz, J.G.** (2009) High-resolution seismic and resistivity profiling of a buried Quaternary subglacial valley: Northern Alberta, Canada. *Geol. Soc. Am. Bull.*, **121**, 1570–1583.

Balco, G., **Rovey, C.W.** and **Stone, J.O.** (2005) The first glacial maximum in North America. *Science*, **307**, 222.

Balleau, W.P. and **Mayer, A.B**. (1988) The transition from ground-water mining to induced recharge in generalized hydrogeologic systems. In: *Proceedings of FOCUS Conference on Southwestern Ground Water Issues*, pp. 81–103. National Water Well Association, Dublin, OH.

Barker, R. and **Harker, D.** (1984) The location of the Stour buried tunnel-valley using geophysical techniques. *Q. J. Eng. Geol. Hydrogeol.*, **17**, 103–115.

Beamish, D. (2003) Airborne EM footprints. *Geophys. Prospect.*, **51**, 49–60.

Best, J.L. and **Ashworth, P.J.** (1997) Scour in large braided rivers and the recognition of sequence stratigraphic boundaries. *Nature*, **387**, 275–277.

Best, M.E., **Levson, V.M.**, **Ferbey, T.** and **McConnell, D.** (2006) Airborne electromagnetic mapping for buried Quaternary sands and in northeast British Columbia, Canada. *J. Environ. Eng. Geophys.*, **11**, 17–26.

Blum, M., **Martin, J.**, **Milliken, K.** and **Garvin, M.** (2013) Paleovalley systems: insights from Quaternary analogs and experiments. *Earth Sci. Rev.*, **116**, 128–169.

Boellstorff, J. (1978a) Chronology of some late Cenozoic deposits from the central United States and the Ice Ages. *Trans. Nebraska Acad. Sci.*, **6**, 35–49.

Boellstorff, J. (1978b) North American Pleistocene stages reconsidered in light of probable Pliocene-Pleistocene glaciation. *Science*, **202**, 305–307.

Boyce, J.I. and **Eyles, N.** (2000) Architectural element analysis applied to glacial deposits: internal geometry of a late Pleistocene till sheet, Ontario, Canada. *Geol. Soc. Am. Bull.*, **112**, 98–118.

Bradwell, T., **Stoker, M.S.**, **Golledge, N.R.**, **Wilson, C.K.**, **Merritt, J.W.**, **Long, D.**, **Everest, J.D.**, **Hestvik, O.B.**, **Stevenson, A.G.** and **Hubbard, A.L.** (2008) The northern sector of the last British Ice Sheet: maximum extent and demise. *Earth Sci. Rev.*, **88**, 207–226.

Carney, C.P., **Abraham, J.D.**, **Cannia, J.C.** and **Steele, G.V**. (2015) Final report on airborne electromagnetic

geophysical surveys and hydrogeologic framework development for the Eastern Nebraska water resources assessment – volume 2, including the Lower Platte North, Lower Platte South, and Nemaha Natural Resources Districts. Exploration Resources International, Vicksburg, MS, 159 pp. Available at: http://www.enwra.org/aem%20data%20download.html (accessed April 19, 2016) at 18:03:00 GMT.

Cummings, D.I., **Russell, H.A.**, **Sharpe, D.R.** and **Fisher, T.G.** (2012) Buried-valley aquifers in the Canadian Prairies: geology, hydrogeology, and origin. *Can. J. Earth Sci.*, **49**, 987–1004.

Cutler, P.M., **Colgan, P.M.** and **Mickelson, D.M.** (2002) Sedimentologic evidence for outburst floods from the Laurentide Ice Sheet margin in Wisconsin, USA: implications for tunnel-channel formation. *Quatern. Int.*, **90**, 23–40.

Denne, J.E., **Yarger, H.L.**, **Macfarlane, P.A.**, **Knapp, R.W.**, **Sophocleous, M.A.**, **Lucas, J.R.** and **Steeples, D.W.** (1984) Remote sensing and geophysical investigations of glacial buried valleys in northeastern Kansas. *Ground Water*, **22**, 56–65.

Divine, D.P. (2014). The Groundwater Atlas of Lancaster County, Nebraska. Resource Atlas 7, Conservation and Survey Division, School of Natural Resources, Institute of Agriculture and Natural Resources, University of Nebraska-Lincoln, Lincoln, NE, 39 pp.

Divine, D.P. and **Korus, J.T**. (2012) *Three-Dimensional Hydrostratigraphy of the Sprague, Nebraska Area: Results from Helicopter Electromagnetic (HEM) Mapping in the Eastern Nebraska Water Resources Assessment (ENWRA).* Geological Survey Bulletin 4 (new series), Conservation and Survey Division, School of Natural Resources, Institution of Agriculture and Natural Resources, University of Nebraska-Lincoln, Lincoln, NE, 32 pp.

Divine, D.P., **Joeckel, R.M.**, **Korus, J.T.**, **Hanson, P.R.** and **Lackey, S.O**. (2009) *Eastern Nebraska Water Resources Assessment (ENWRA): Introduction to a Hydrogeologic Study* Conservation Bulletin 1 (new series). Conservation and Survey Division, School of Natural Resources, Institute of Agriculture and Natural Resources, University of Nebraska-Lincoln, Lincoln, NE, 31 pp.

Dreeszen, V.H. (1970) The stratigraphic framework of Pleistocene glacial and periglacial deposits in the Central Plains. In: *Pleistocene and Recent Environments of the Central Great Plains* (Eds W. Dort and J. Knox Jones), Special Publication 3, pp. 9–22. Department of Geology, University of Kansas, Lawrence, KS.

Dreeszen, V.H. and **Burchett, R.R**. (1971) Buried valleys in the lower part of the Missouri River Basin. In: *Pleistocene Stratigraphy of Missouri River Valley along the Kansas-Missouri Border* (Eds C.K. Bayne, H.G. O'Connor, S.N. Davis and W.B. Howe), Special Publication 53, pp. 21–25. Kansas Geological Survey, Lawrence, KS.

Druliner, A.D. and **Mason, J.P**. (2001) Hydrogeology and water quality of five principal aquifers in Lower Platte South Natural Resources District, eastern Nebraska. U.S. Geological Survey Water Resources Investigation 00-4155, 45 pp.

Emery, P.A. (1966) Geohydrology of Saline County, Nebraska. U.S. Geological Survey Hydrologic Investigations Atlas HA-216, 5 pp, 1 map sheet.

Farquharson, C.G., **Oldenberg, D.W.** and **Routh, P.S.** (2003) Simultaneous one-dimensional inversion of loop-loop electromagnetic data for magnetic susceptibility and electrical conductivity. *Geophysics*, **68**, 1857–1869.

Fenneman, N.M. (1946) Physical divisions of the United States. U.S. Geological Survey map, scale 1:7,000,000, 1 sheet.

Fielding, C.R. (2007) Sedimentology and stratigraphy of large river deposits: recognition in the ancient record, and distinction from "incised valley fills". In: *Large Rivers: Geomorphology and Management* (Ed. A. Gupta), pp. 97–114. John Wiley & Sons Ltd, Chichester.

Fisher, T.G. and **Taylor, L.D.** (2002) Sedimentary and stratigraphic evidence for subglacial flooding, south-central Michigan, USA. *Quatern. Int.*, **90**, 87–115.

Fisher, T.G., **Jol, H.M.** and **Boudreau, A.M.** (2005) Saginaw Lobe tunnel channels (Laurentide Ice Sheet) and their significance in south-central Michigan, USA. *Quatern. Sci. Rev.*, **24**, 2375–2391.

Gabriel, G., **Kirsch, R.**, **Siemon, B.** and **Wiederhold, H.** (2003) Geophysical investigation of buried Pleistocene subglacial valleys in Northern Germany. *J. Appl. Geophys.*, **53**, 159–180.

Galloway, W.E., **Whiteaker, T.L.** and **Ganey-Curry, P.** (2011) History of Cenozoic North American drainage basin evolution, sediment yield, and accumulation in the Gulf of Mexico basin. *Geosphere*, **7**, 938–973.

Gibling, M.R. (2006) Width and thickness of fluvial channel bodies and valley fills in the geological record: a literature compilation and classification. *J. Sed. Res.*, **76**, 731–770.

Ginsberg, M.H. (1983) *Hydrogeology of Butler County, Nebraska*. Conservation and Survey Division, Institute of Agriculture and Natural Resources, University of Nebraska-Lincoln, Lincoln, NE, 78 pp.

Goodenkauf, O. (1978) The groundwater geology of southern Lancaster County, Nebraska. Unpublished MS Thesis, Department of Geology, University of Nebraska-Lincoln, Lincoln, NE, 117 pp.

Gosselin, D.C., **Headrick, J.**, **Tremblay, R.**, **Chen, X.-H.** and **Summerside, S.E.** (1997) Domestic well water quality in rural Nebraska, focus on nitrate-nitrogen, pesticides, and coliform bacteria. *Groundwater Monit. Remediat.*, **17**, 77–87.

Heim, G.E. and **Howe, W.B.** (1963) Pleistocene drainage and depositional history in northwestern Missouri. *Trans. Kansas Acad. Sci.*, **66**, 378–392.

Hooke, R.L. and **Jennings, C.E.** (2006) On the formation of the tunnel valleys of the southern Laurentide ice sheet. *Quatern. Sci. Rev.*, **25**, 1364–1372.

Howe, W.B. (1968) *To Pleistocene and Pennsylvanian Formations in the St. Joseph area, Missouri*. Missouri Geological Survey and Water Resources, Rolla, MO, 45 pp.

Høyer, A.-S., **Jørgensen, F.**, **Sandersen, P.**, **Viezzoli, A.** and **Møller, I.** (2015) 3D geological modelling of a complex buried-valley network delineated from borehole and AEM data. *J. Appl. Geophys.*, **122**, 94–102.

Huuse, M. and **Lykke-Andersen, H.** (2000) Overdeepened Quaternary valleys in the eastern Danish North Sea: morphology and origin. *Quatern. Sci. Rev.*, **19**, 1233–1253.

Janszen, A., **Moreau, J.**, **Moscariello, A.**, **Ehlers, J.** and **Kröger, J.** (2013) Time-transgressive tunnel-valley infill revealed by a three-dimensional sedimentary model, Hamburg, north-west Germany. *Sedimentology*, **60**, 693–719.

Joeckel, R.M. and **Dillon, J.S**. (2007a) Surficial Geology of the Cortland 7.5 Minute Quadrangle, Nebraska. Conservation and Survey Division, School of Natural Resources, University of Nebraska-Lincoln, scale 1:24,000, 1 sheet.

Joeckel, R.M. and **Dillon, J.S**. (2007b) Surficial Geology of the Firth 7.5 Minute Quadrangle, Nebraska. Conservation and Survey Division, School of Natural Resources, University of Nebraska-Lincoln, scale 1:24,000, 1 sheet.

Joeckel, R.M. and **Howard, L.M**. (2009) Surficial Geology of the Hallam 7.5 Minute Quadrangle, Nebraska. Conservation and Survey Division, School of Natural Resources, University of Nebraska-Lincoln, scale 1:24,000, 1 sheet.

Joeckel, R., **Loope, H.**, **Wally, K.** and **Hellerich, J.** (2007) Late Cenozoic geomorphology of a bedrock-dominated landscape adjacent to the Laurentide glacial limit: southeastern Nebraska, USA. *Z. Geomorphol.*, **51**, 469–486.

Jørgensen, F. and **Sandersen, P.B.E.** (2006) Buried and open tunnel valleys in Denmark—erosion beneath multiple ice sheets. *Quatern. Sci. Rev.*, **25**, 1339–1363.

Jørgensen, F., **Lykke-Andersen, H.**, **Sandersen, P.B.**, **Auken, E.** and **Nørmark, E.** (2003) Geophysical investigations of buried Quaternary valleys in Denmark: an integrated application of transient electromagnetic soundings, reflection seismic surveys and exploratory drillings. *J. Appl. Geophys.*, **53**, 215–228.

Keech, C.F., **Dreeszen, V.H.** and **Emery, P.A**. (1967) Availability of Ground Water in York County, Nebraska. U.S. Geological Survey Water Supply Paper 1839-F, 17 pp.

Kehew, A.E. and **Boettger, W.M.** (1986) Depositional environments of buried-valley aquifers in North Dakota. *Groundwater*, **24**, 728–734.

Kehew, A.E., **Piotrowski, J.A.** and **Jørgensen, F.** (2012) Tunnel valleys: concepts and controversies—a review. *Earth Sci. Rev.*, **113**, 33–58.

Kehew, A.E., **Ewald, S.K.**, **Esch, J.M.** and **Kozlowski, A.L.** (2013) On the origin of tunnel valleys of the Saginaw Lobe of the Laurentide Ice Sheet; Michigan, USA. *Boreas*, **42**, 442–462.

Kirsch, R. (2009) *Groundwater Geophysics: A Tool for Hydrogeology*. Springer-Verlag, Berlin, 548 pp.

Kjær, K.H., **Sultan, L.**, **Krüger, J.** and **Schomacker, A.** (2004) Architecture and sedimentation of outwash fans in front of the Mýrdalsjökull ice cap, Iceland. *Sed. Geol.*, **172**, 139–163.

Korus, J.T. and **Burbach, M.E.** (2009) Analysis of aquifer depletion criteria with implications for groundwater management. *Great Plains Res.*, **19**, 187–200.

Korus, J.T., **Joeckel, R.M.** and **Divine, D.P**. (2013) *Three-Dimensional Hydrostratigraphy of the Firth, Nebraska Area: Results from Helicopter Electromagnetic (HEM) mapping in the Eastern Nebraska Water Resources Assessment (ENWRA)*. Geological Survey Bulletin 3 (new series), Conservation and Survey Division, School of Natural Resources, Institute of Agriculture and Natural Resources, University of Nebraska-Lincoln, Lincoln, NE, 100 pp.

Kristensen, T.B., **Huuse, M.**, **Piotrowski, J.A.** and **Clausen, O.R.** (2007) A morphometric analysis of tunnel valleys in the eastern North Sea based on 3D seismic data. *J. Quatern. Sci.*, **22**, 801–815.

Lanphere, M.A., **Champion, D.E.**, **Christiansen, R.L.**, **Izett, G.A.** and **Obradovich, J.D**. (2002) Revised ages for tuffs of the Yellowstone Plateau volcanic field — assignment of the Huckleberry Ridge Tuff to a new geomagnetic polarity event. *Geo. Soc. Am. Bull.*, **114**, 559–568.

Lesmes, D.P. and **Friedman, S.P**. (2005) Relationship between the electrical and hydrogeological properties of rocks and soils. In: *Hydrogeophysics* (Eds Y. Rubin and S.S. Hubbard), pp. 87–128. Springer-Dordrecht, The Netherlands.

Ley-Cooper, Y. and **Davis, A**. (2010) Can a borehole conductivity log discredit a whole AEM survey? ASEG Extended Abstracts, 1–5.

Lohman, S.W. (1972) Ground-Water Hydraulics. U.S. Geological Survey Professional Paper 708, 70 pp.

Lugn, A.L. (1935) The Pleistocene geology of Nebraska. Nebraska Geological Survey Bulletin 10. Conservation and Survey Division, University of Nebraska-Lincoln, Lincoln, NE, 223 pp.

Marren, P.M., **Russell, A.J.** and **Rushmer, E.L.** (2009) Sedimentology of a sandur formed by multiple jökulhlaups, Kverkfjöll, Iceland. *Sed. Geol.*, **213**, 77–88.

Maxey, G.B. (1964) Hydrostratigraphic units. *J. Hydrol.*, **2**, 124–129.

Palacky, G.J. and **Stevens, L.E.** (1990) Mapping of Quaternary sediments in northeastern Ontario using ground electromagnetic methods. *Geophysics*, **55**, 1595–1604.

Piotrowski, J.A. (1994) Tunnel-valley formation in northwest Germany – geology, mechanisms of formation and subglacial bed conditions for the Bornhoved tunnel valley. *Sed. Geol.*, **89**, 107–141.

Piotrowski, J.A. (1999) Channelized subglacial drainage under soft-bedded ice sheets: evidence from small N-channels in Central European Lowland. *Geol. Q.*, **43**, 153–162.

Pugin, A.J.-M., **Oldenborger, G.A.**, **Cummings, D.I.**, **Russell, H.A.** and **Sharpe, D.R.** (2014) Architecture of buried valleys in glaciated Canadian Prairie regions based on high resolution geophysical data. *Quatern. Sci. Rev.*, **86**, 13–23.

Räsänen, M., **Auri, J.**, **Huitti, J.**, **Klap, A.** and **Virtasalo, J.** (2009) A shift from lithostratigraphic to allostratigraphic classification of Quaternary glacial deposits. *GSA Today*, **19**, 4–11.

Reed, E.C. and **Dreeszen, V.H**. (1965) Revision of the classification of the Pleistocene deposits of Nebraska. Geological Survey Bulletin 23, Conservation and Survey Division, University of Nebraska-Lincoln, Lincoln, NE, 65 pp.

Reid, J.E. and **Vrbancich, J.** (2004) A comparison of the inductive-limit footprints of airborne electromagnetic configurations. *Geophysics*, **69**, 1229–1239.

Reid, J.E., **Pfaffling, A.** and **Vrbancich, J.** (2006) Airborne electromagnetic footprints in 1D earths. *Geophysics*, **71**, G63–G72.

Robinson, D.A., **Binley, A.**, **Crook, N.**, **Day-Lewis, F.D.**, **Ferre, T.P.A.**, **Grauch, V.J.S.**, **Knight, R.**, **Knoll, M.**, **Lakshmi, V.**, **Miller, R.**, **Nyquist, J.**, **Pellerin, L.**, **Singha, K.** and **Slater, L.** (2008) Advancing process-based watershed hydrological research using near-surface geophysics: a vision for, and review of, electrical and magnetic geophysical methods. *Hydrol. Process.*, **22**(18), 3604–3635.

Roy, M., **Clark, P.U.**, **Barendregt, R.W.**, **Glasmann, J.R.** and **Enkin, R.J.** (2004) Glacial stratigraphy and paleomagnetism of late Cenozoic deposits of the north-central United States. *Geological Society of America Bulletin*, **116**, 30–41.

Russell, H.A.J., **Hinton, M.J.**, **Van der Kamp, G.** and **Sharpe, D.R**. (2004) An overview of the architecture, sedimentology and hydrogeology of buried-valley aquifers in Canada. In: *57th Canadian Geotechnical Conference and the 5th joint CGSIAH Conference, Quebec, Canada; October 24–27, 2004*. Geological Survey of Canada, Contribution Series 2004085; Earth Sciences Sector, General Information Product 27, pp. 26–33.

Russell, A.J., **Roberts, M.J.**, **Fay, H.**, **Marren, P.M.**, **Cassidy, N.J.**, **Tweed, F.S.** and **Harris, T.** (2006) Icelandic jökulhlaup impacts: implications for ice-sheet hydrology, sediment transfer and geomorphology. *Geomorphology*, **75**, 33–64.

Sandersen, P.B., **Jørgensen, F.**, **Larsen, N.K.**, **Westergaard, J.H.** and **Auken, E.** (2009) Rapid tunnel-valley formation

beneath the receding Late Weichselian ice sheet in Vendsyssel, Denmark. *Boreas*, **38**, 834–851.

Seaber, P.R. (1988) Hydrostratigraphic units. In: *Hydrogeology, The Geology of North America* (Eds W. Back, J.S. Rosenshein and P.R. Seaber), O-2, pp. 9–14. Geological Society of America, Boulder, CO.

Shaver, R.B. and **Pusc, S.W.** (1992) Hydraulic barriers in Pleistocene buried-valley aquifers. *Ground Water*, **30**, 21–28.

Slomka, J.M., **Eyles, C.H.**, **Mulligan, R.P.M.**, **McKay, E.D.** and **Berg, R.C.** (2015) Internal architecture of a till sheet, Tiskilwa Formation, north-central Illinois, USA: application of architectural element analysis. *Sedimentology*, **62**, 1328–1359.

Smith, N.D. (1985) Proglacial fluvial environment. In: *Glacial Sedimentary Environments* (Eds G.M. Ashley, J. Shaw and N.D. Smith), Short course 16, pp. 85–134. SEPM, Tulsa, OK.

Smith, B.D., **Abraham, J.D.**, **Cannia, J.C.**, **Steele, G.V.** and **Hill, P.L**. (2008) Helicopter electromagnetic and magnetic geophysical survey data, Oakland, Ashland, and firth study areas, Eastern Nebraska, March 2007. US Geological Survey Open-File Report 2008-1018, 16 pp.

Smith, B.D., **Abraham, J.D.**, **Cannia, J.C.**, **Minsley, B.J.**, **Ball, L.B.**, **Steele, G.V.** and **Deszcz-Pan, M**. (2011) Helicopter electromagnetic and magnetic geophysical survey data, Swedeburg and Sprague study areas, eastern Nebraska, May 2009. U.S. Geological Survey Open-File Report 2010-1288, 37 pp.

Stanley, K.O. and **Wayne, W.J.** (1972) Epeirogenic and climatic controls of Early Pleistocene fluvial sediment dispersal in Nebraska. *Geol. Soc. Am. Bull.*, **83**, 3675–3690.

Steuer, A., **Siemon, B.** and **Auken, E.** (2009) A comparison of helicopter-borne electromagnetics in frequency-and time-domain at the Cuxhaven valley in Northern Germany. *J. Appl. Geophys.*, **67**, 194–205.

Todd, J.E. (1911) History of Wakarusa Creek. *Trans. Kansas Acad. Sci.*, **23**(24), 211–218.

U.S. Geological Survey (2015) *USGS NED: U.S.* Geological Survey, Reston, VA. http://ned.usgs.gov/;http://nationalmap.gov/viewer.html (accessed on November 16, 2015).

van der Vegt, P., **Janszen, A.** and **Moscariello, A.** (2012) Tunnel valleys: current knowledge and future perspectives. *Geol. Soc. London Spec. Publ.*, **368**, 75–97.

Viezzoli, A., **Christiansen, A.V.**, **Auken, E.** and **Sørensen, K.** (2008) Quasi-3D modeling of airborne TEM data by spatially constrained inversion. *Geophysics*, **73**, F105–F113.

Witzke, B.J. and **Ludvigson, G.A**. (1990) Petrographic and stratigraphic comparisons of sub-till and inter-till alluvial units in western Iowa; implications for development of the Missouri River drainage. In: *Holocene Alluvial Stratigraphy and Selected Aspects of the Quaternary History of Western Iowa* (Ed. E.A.I. Bettis), Midwest Friends of the Pleistocene 37th Field Conference, Guidebook Series 9, pp. 119–143. Iowa Geological Survey, Iowa City, IA.

Yin, C., **Huang, X.**, **Liu, Y.** and **Cai, J.** (2014) Footprint for frequency-domain airborne electromagnetic systems. *Geophysics*, **79**, E243–E254.

Manuscript received 4 January 2016; revision accepted 20 July 2016